Functionalized Hexagonal Boron Nitride Nanosheets/PMMA Nanocomposites for Structural Applications

By

Muhammad Umer Farooq

School of Chemical and Materials Engineering

National University of Sciences and Technology

Islamabad, Pakistan

2019

Functionalized Hexagonal Boron Nitride Nanosheets/PMMA Nanocomposites for Structural Applications

Muhammad Umer Farooq

00000172641

This thesis is submitted as a partial fulfillment of the requirements for the degree of MS in Materials and Surface Engineering

Supervisor Name: Dr. Usman Liaqat

School of Chemical and Materials Engineering (SCME)

National University of Sciences and Technology (NUST)

H-12, Islamabad, Pakistan

October, 2019

THESIS ACCEPTANCE CERTIFICATE

Certified that final copy of MS thesis written by Mr. **Muhammad Umer Farooq** (Registration No 00000172641), of School and Chemical & Materials Engineering (SCME) has been vetted by undersigned, found complete in all respects as per NUST Statues/Regulations, is free of plagiarism, errors, and mistakes and is accepted as partial fulfillment for award of MS degree. It is further certified that necessary amendments as pointed out by GEC members of the scholar have also been incorporated in the said thesis.

Signature: _____

Name of Supervisor: **Dr Usman Liaqat** _____

Date: _____

Signature (HOD): _____

Date: _____

Signature (Dean/Principal): _____

Date: _____

Form TH-1

(Must be type written)

National University of Sciences & Technology (NUST)
MASTER'S THESIS WORK
Formulation of Guidance and Examination Committee (GEC)

Name: Muhmmad Umer Farooq   NUST Regn No: 00000172641

Department: Material Engineering   Specialization: MS Material and Surface Engineering

Credit Hour Completed: (09) 24   GPA/CGPA: (3.67) 3.81

Course Work Completed

S/No	Code	Title	Core/Elective	CH	Grade
1	MSE-811	Material Thermodynamics	Core	3	B+
2	MSE-821	Mechanical Behavior of Materials	Core	3	A
3	MSE-871	Polymer Engineering	Elective	3	B+

Date 22-05-17   Student's Signature _____

Thesis Committee

1. Name: Dr.Usman Liaqat (Supervisor)
   Signature: _____
   Department: Material Enginnering
2. Name: Dr.Ahmad Nawaz Khan (Co-Supervisor)
   Signature: _____
   Department: Material Enginnering
3. Name: Dr.Iftikhar H. Gul
   Signature: _____
   Department: Material Enginnering
4. Name: Dr. Rahim Jan (External)
   Signature: _____
   Department: NESCOM

Date: 22/5/17   Signature of Head of Department: _____

APPROVAL

Date: _____   Dean/Principal _____

Distribution

1x copy to Exam Branch, Main Office NUST
1x copy to PGP Dte, Main Office NUST
1x copy to Exam branch, respective institute

School of Chemical and Materials Engineering (SCME) Sector H-12, Islamabad

	Code	Title	Core/Elective	CH	Grade
4	MSE-812	Phase Transformation and Microstructures	Core	3	A
	MSE-851	Surface Engineering and Characterization	Core	3	A
	MSE-862				

FORM TH-4

MASTER'S THESIS WORK

We hereby recommend that the dissertation prepared under our supervision by Regn No & Name: 00000172641 Muhammad Umer Farooq

Title: **Functionalized Hexagonal Boron Nitride Nanosheets/PMMA Nanocomposites for Structural Applications.**

Presented on: **03 Oct 2019**   at: **1400 hrs in SCME Seminar Hall**

Be accepted in partial fulfillment of the requirements for the award of Masters of Science degree in **Materials & Surface Engineering**.

Guidance & Examination Committee Members

Name: **Dr Rahim Jan** (External)   Signature: _____

Name: **Dr Iftikhar Hussain Gul**   Signature: _____

Name: **Dr Malik Adeel Umer**   Signature: _____

Supervisor's Name: **Dr Usman Liaqat**   Signature: _____
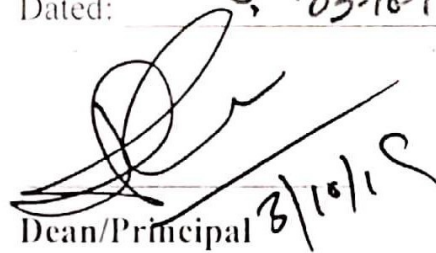
Dated: 03-10-19

Head of Department

Date 3/10/19

Dean/Principal 3/10/19

Date _____

School of Chemical &Materials Engineering (SCME)

DEDICATION

I dedicate this thesis to my loving Mother and caring Father

ACKNOWLEGEMENTS

Abstract

Till date, dispersion of nanofillers in polymer matrices remains a major challenge. Functionalization of nano-reinforcements prior to mixing is amongst the different ways to improve their dispersion and enhance their overall effect. In this study, hydroxylated functionalized hexagonal boron nitride nanosheets (h-BNNSs-OH) were prepared by hydroxylated assisted exfoliation for improved dispersion. Fourier transform infra-red, FTIR, spectroscopy was used to confirm of the presence of functional groups on h-BN. Polymer nanocomposites were prepared using hydroxyl (OH) functionalized and non-functionalized BNNSs with poly methyl methacrylate, PMMA, by solution mixing for comparative study. Structural and morphological characteristics were analyzed using X-ray Diffraction, XRD and scanning electron microscopy (SEM) respectively. Dimensional analysis of nanosheets was carried out using atomic force microscopy (AFM). Differential scanning calorimeter was used to study the polymer and nanosheets interactions. Mechanical behavior of the composites was studied by utilizing tensile testing. It was observed that tensile strength, Young's modulus and strain at break of nanocomposites enhanced significantly. These nanocomposites can be used as a structural component for automobiles, unmanned aircrafts, construction, infrastructures and drone technology.

Table of Contents

List of Figures

List of Table

List of Abbreviations

h-BN _____ Hexagonal Boron Nitride

h-BNNS-OH _____ Hexagonal Boron Nitride Nanosheets
Functionalized with Hydroxylic group

PMMA _____ Poly- (methyl methacrylate)

CNTs _____ Carbon Nanotubes

DMF _____ Dimethylformamide

IPA _____ Isopropyl Alcohol

NMP _____ N-Methyl-2-Pyrrolidone

SAE _____ Sonication Assisted Exfoliation

SDC _____ Sodium Deoxy Cholate

XRD _____ X-Ray Diffraction

SEM _____ Scanning Electron Microscopy

AFM _____ Atomic Force Microscopy

FTIR _____ Fourier Transform Infrared

DSC_____ Differential Scanning Calorimetry

Chapter: 1

Introduction

"A wave of innovative flat materials is following in the wake of graphene."

Gibnery E. [1]

The discovery of graphene opened a new branch for materials science as 2D nanomaterials. These 2D materials are crystalline layered materials. There is potential for 500 other materials like graphene [1]. Graphene possesses many exceptional properties like thermal and electrical conductivity, outstanding mechanical strength, high chemical and thermal stability at higher temperatures. That is why it found its applications in electronics, supercapacitors, nanocomposites, bioengineering, energy storage and photovoltaics [2]. It was estimated that by 2025 the market size for graphene will reach up to USD 550 million [3].

Taking graphene into account, other 2D materials have also been explored, one of which is hexagonal boron nitride nanosheets (h-BNNSs). It has the similar structure as that of graphene that is why h-BNNS is also referred to as white graphene. It has similar properties as of graphene with few exceptions such as it has better thermal stability and has wide band gap which makes it insulator. That is why it has found its use in various applications [4]. The analysts showed that market for h-BN will grow at a rate of 5.4% annually from 2019-2023 [5].

In the recent years, the study of polymers reinforced by two-dimensional materials have seen resurgence in the area of polymer nanocomposites. The addition of these two-dimensional materials in polymers has shown a tremendous enhancement in the properties of polymers such as thermal, mechanical and electrical properties [6].

1.1 Nanocomposites

Nanocomposites are a type of composite which have one phase in the nanometer scale. These nanocomposite shows exceptional properties with the combination of various design possibilities and high performance that is why they are said to be the 21st century materials. The nanocomposites are grouped based on the matrix part of the composite. The matrix part can either be metal, ceramic or polymer. This study is focused on polymer nanocomposite. The final macroscopic and microscopic properties and performance of these polymer nanocomposite is the characteristic effect of nano-

filler, polymer-filler interface. The potential of these polymer nanocomposites is promising in various applications from packing materials to biomaterials.

Literature review shows that there are more than 18,000 research publications that have been available online from the last two decades. It has been evidenced that the material's property can change drastically at nanometer scale (<100 nm). The reduction in material size can achieve new properties like enhancement in strength, elasticity, electrical and thermal conductivity, insulation and even reactivity that the materials don't show at macro or even micrometer scale.

1.2   Nano Fillers

The properties of nanocomposites not only change by the intrinsic characteristics of nanofiller, but also on the shape and size of these nano-fillers. There are three different geometries of nanofillers that are used in nanocomposites [7].

- Zero-dimensional (nanoparticles, quantum dots)
- One-dimensional (nanofibers, nanotubes, nanorods)
- Two-dimensional (nanosheets, nanoplatelets)

In this study two-dimensional nanosheets are used as they have highest surface to volume ratio.
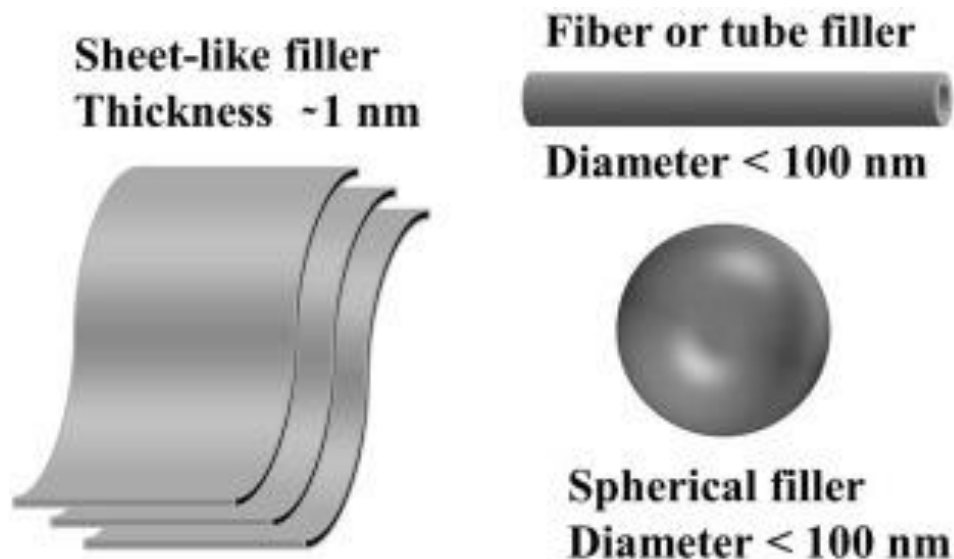
Figure 1-1: Three different geometries of nanofillers [7]

1.3   Structural Application of Nanocomposites

All structural applications require high strength, durability, toughness and stiffness. For these applications, the metals, ceramics and their composites are the best choice.

But there are significant challenges like lighter weight materials are required at low cost that are corrosion resistant and easy to process. For structural applications, such as construction, automobile, aircraft, infrastructure, drone technology and space, the lightweight materials are the main requirement for economical in cost and energy. Polymer are then better choice as they excel in low cost, low density, corrosion resistance and easy processing. But their strength and stiffness are the major concern for structural applications. That is where polymer composite comes in [8].

The polymer composites demand high loading of fillers to reach the desired strength and other applications. The nanofillers have high surface area which will increase the polymer and reinforcement interfacial area and can give desired properties even at low loading of 0.5-2 %. But nanofillers pose another problem of dispersion in polymer matrix [9].

1.4 Thesis Outline

The motivation of this study is to address the issue of poor interaction between polymers and BNNSs that lead to aggregation and lower the required properties. We functionalized the boron nitride nanosheets to overcome this issue to achieve required properties. The mechanical behavior and thermal characteristics have been studied to comprehend how functionalized boron nitride nanosheets affect the properties of nanocomposites. The short introduction of polymers and nanosheets and their production methods have been highlighted in chapter 2, the detail of experimental methods is discussed in chapter 3, followed by characterization technique used to analyze in chapter 4, results and discussions are stated in chapter 5 along with conclusions and future recommendations.

Chapter: 2

Literature Review

This chapter will provide the brief review of polymer nanocomposites, their fundamentals, and processing of nanocomposites.

2.1 Basics of Polymer Nanocomposites

2.1.1 Polymer Matrix

Polymers can be categorized based on their physical properties:

- Rigid plastics
- Elastomers

Rigid plastics are of two types' thermoplastics and thermosets. The thermoplastics consists of long chains either linear, branched or cyclic. These chains are linked by covalent bonds. They are heat reversible. On the other hand, thermosetting polymers are highly crosslinked and have network structure. They are heat irreversible. Elastomers are stretchable polymers like rubbers. They are elastic in nature. There is another class of polymer that can be obtained by combining rigid thermoplastics and elastomer: thermoplastic elastomer [10].
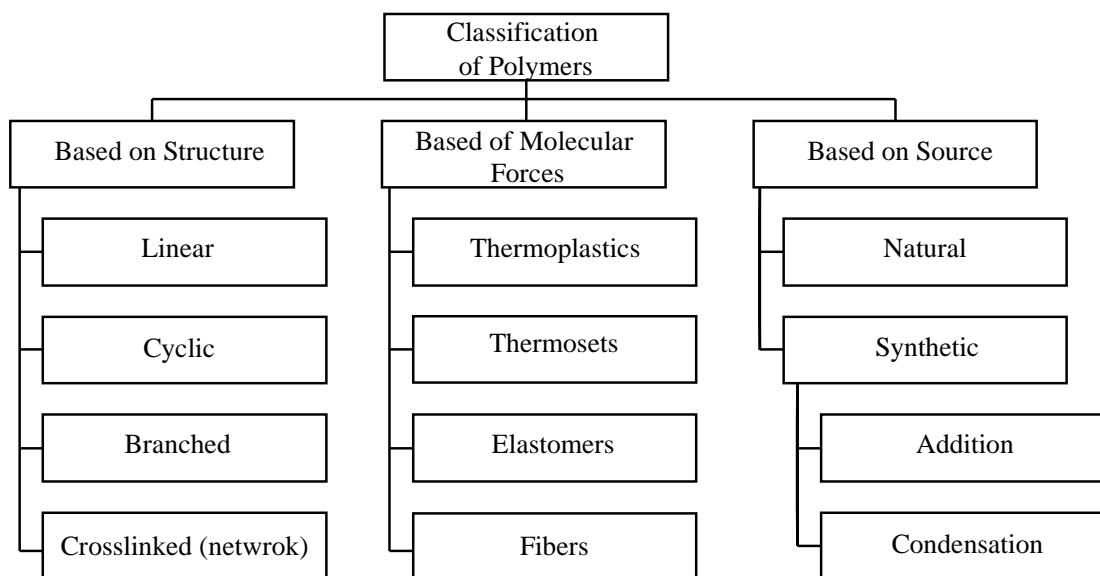
Figure 2-1: Classification of polymers [10]

In this study poly- (methyl methacrylate) (PMMA) is used as a polymer matrix. PMMA is an amorphous glassy polymer. Because it is amorphous in nature (to avoid complexity of crystallization) and it is suitable for various processing and production

methods [11]. PMMA has enormous applications and end-use environmental potential that is why many researchers are utilizing PMMA for various nanocomposites studies to improve its mechanical and thermal properties [10].
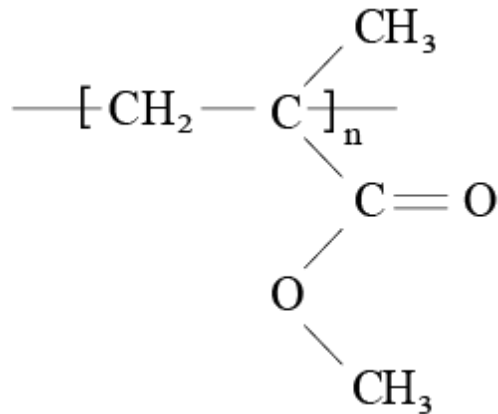
Figure 2-2: Structure of PMMA

PMMA goes in the category of polymers that are amorphous in nature. These polymers do not crystallize while cooling as their structure has rigid backbone. The thermal transitions that are of utmost importance are glass transition temperature known as T_g. The glass transition temperature is the temperature above which polymer shows rubbery behavior and below which it behaves as a gassy material. In dynamic mechanical testing T_g can be obtained using storage and loss modulus. The polymers that has T_g above room temperature shows stiff and brittle behavior at room temperature while the polymers have T_g less than room temperature shows rubbery behavior and are soft and flexible at room temperature. The T_g of PMMA is ~ 100 °C [12].

2.1.2 Polymer Reinforcement

Reinforcements are additives or fillers, added into the polymer for various applications to improve its processing, properties or simply to add color. These reinforcements allow polymers to give required properties based on the type of reinforcement added for required applications. As the demand of PMMA is high for various applications, these reinforcements are added to improve its thermal and mechanical properties. With current technological advancements in polymer composites, more and more research focus is shifting toward nano reinforcements. The advantage of nano reinforcements is that polymers shows superior properties without compromising its processing conditions. Nano reinforcements have one dimension in nanoscale (1-100 nm). As the

size reduces it creates large interfacial area for reinforcements to interact with polymers to increase overall performance [13, 14].

The use of graphene (2-dimensional) in polymers shows extraordinary properties. Now researchers are exploring other 2-dimensional nano materials such as MoS_2, WS_2, BN etc. In this study h-BN nanosheets are used to investigate its effect on PMMA. Boron nitride exhibits superior thermal, mechanical and electrical properties and incorporating in polymers lead to enhance nanocomposite properties [15]. The use of these nanomaterials at low loadings can achieve desired properties for nanocomposites [16].

2.1.3 Polymer Nanocomposite

Polymer nanocomposites consists of two parts; polymer matrix and nano reinforcement (having one dimension less than 100 nm). Polymer nanocomposites in recent years have become very important field for research because by adding very small amounts of reinforcements (<5%) polymers can achieve the desired properties. Like simple polymer composite, polymer-reinforcement interface plays an important role. The interface is the region of reinforcement and polymer boundary where properties of polymers changes. The two major features that control the properties and performance of these polymer nanocomposites are properties at interface and their resulting changes in the nanocomposite [16].

2.2 Preparation Methods of Polymer Nanocomposites

The preparation processes of nanocomposites play significant effect on the properties of bulk nanocomposites. The dispersion of h-BN in polymers is an essential factor for optimizing the performance of nanocomposites. The following are some techniques used to prepare these nanocomposites.

2.2.1 Melt Mixing

Melt mixing is most commonly adopted technique for industrial processes. This method involves mixing of polymer matrix with nanosheets in melt form at higher temperature and higher shear forces. The benefit of this method is, the solvent is not required during processing. This method is suitable when loading of 1-10 wt. % nanoparticles is required. Because as the nanoparticle concentration increases, the viscosity of polymer increases, and the processing becomes more difficult. Wu H. and Kessler MR. fabricated h-BN/bisphenol E cyanate ester nanocomposites using melt mixing at 130 °C. Then cured at 180 °C and

250°C [17]. Xie *et al* prepared nanocomposites using liquid exfoliated BNNSs with poly (ethylene terephthalate) by melt mixing and reported enhanced barrier properties [18]. Different researchers then tried to obtain nanocomposite by incorporating solution mixing and melt mixing in two-step process. Wu *et al*. used slurry compounding method using two roll-mill to prepare BNNS/SBR thermal conductive nanocomposite [19]. Haggenmueler et al. used a combination of both methods to form aligned CNT/polymer nanocomposite [20].

2.2.2 Solution Mixing

In this method both, the nanosheets and polymer are dispersed in solvent (to make low viscosity mixture). These nanosheets and polymer solution are dispersed using stirring and ultrasonication. The dispersed mixture is casted on glass slide or petri dish and thin film is obtained by evaporation. In this technique, the use of solvent is very important, as it is necessary that the polymers can be easily dissolved in solvent and suitable for making nanosheet suspensions. Many polymer nanocomposites were prepared using solution mixing. Liu, F. *et al* fabricated h-BN nanosheets/PMMA nanocomposite using solution mixing and use DMF as solvent for enhanced mechanical properties [21]. Ye, H. *et al* prepared h-BN/HBPE nanocomposite by solution mixing using chloroform as solvent to study dielectric properties [22]. Yu, J. *et al* prepared h-BN nanosheets/epoxy nanocomposite using this method for thermal conductive and dielectric properties [23]. Gonzalez. O. *et al* prepared h-BNNS/PVA porous membranes [24]. This technique is for those polymers only which are soluble in suitable solvents.

2.2.3 In-situ Polymerization

The high loading of nanosheets would reduce the mechanical properties of nanocomposites as nanosheets can agglomerate or stacked at high loading. Thus in-situ polymerization technique was developed to address this issue. This technique involves dispersion of nanosheets in monomers and then polymerized the mixture.

Using this method high interface bonding between nanosheets and polymer chain can be obtained. In this technique the functionalized nanosheets form covalent bonds with polymer matrix during chemical reaction. Huang, X. *et al* fabricated h-BNNS/PS nanocomposite by polymerization of styrene monomers with modified BNNSs [25]. Qin *et al* prepared h-BN/PMMA nanocomposite by bulk polymerization of dispersed boron nitride in methyl methacrylate monomers [26]. A distinctive approach was

followed by Lee *et al*, they grafted polycaprolactone on BNNSs and then followed by ring opening polymerization of grafted polycaprolactone and they reported the thermal properties of polymer nanocomposites [27]. The downsides of this method are that there are a lot of parameters to control to obtain reproducible and consistent nanocomposites such as initiator concentration, solvent content and amount of stirring to disperse the nanosheets and polymerization time and temperature [27].

2.2.4 Polymer Grafting

Nanosheets can be utilized in in-situ polymerization to form nanocomposite but sometimes there is less interaction between nanosheets and monomers to obtain required dispersion. To overcome this problem, the nanosheets can be first functionalized and then dispersed with monomers to start in-situ polymerization. In this method, the covalent functionalization of nanosheets with in-situ polymerization is called polymer grafting. This method of preparing nanocomposite has demonstrated that successful nanocomposite with enhanced dispersion and excellent mechanical properties can be achieved [28].

2.3 Hexagonal Boron Nitride Nanosheets (h-BNNSs)

Two dimensional materials with layered structure are crystalline in nature. The hexagonal boron nitride nanosheets (h-BNNSs) being the one is analogous to graphene with equal number of B and N atoms in its structure. In 1991 [29], after the discovery of carbon nanotubes (CNTs), in 1995 [30], boron nitride nanotubes (BNNTs) were successfully prepared. The other boron nitride nanomaterials were prepared like, nano-fibers and nano-rods. In 1998 [31-33], they tried to prepare boron nitride fullerene (octahedral) like fullerene of carbon (Bucky ball) by Stephen and Golberg. In 2004, Andre Geim and Konstantin Novoselov discovered graphene, which revolutionized the science in 2-d materials. h-BN being one of them [34].
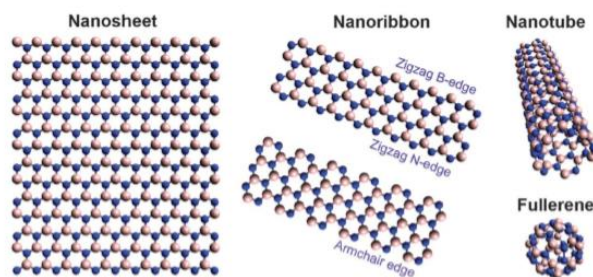
Figure 2-3: 0D, 1D and 2D boron nitride nanomaterials [35]

2.3.1   Structure

Boron nitride nanosheets have a hexagonal structure analogous to graphene, in which atoms of boron are covalently bonded with other three atoms of nitrogen and vice versa. BNNSs has a strong bonding in-plane bonding (covalent) and weak out-of-plane bonding (van der Waals forces). This results in 3-dimensional structures. The bond length of B-N is around 1.45 Å. The planes are around 3.3 Å apart. Boron nitride thus, has a layered structure as of graphite. The stacking of planes in h-BN is different as compared to graphite. The h-BN has AÁ sacking while graphite has AB stacking [36].
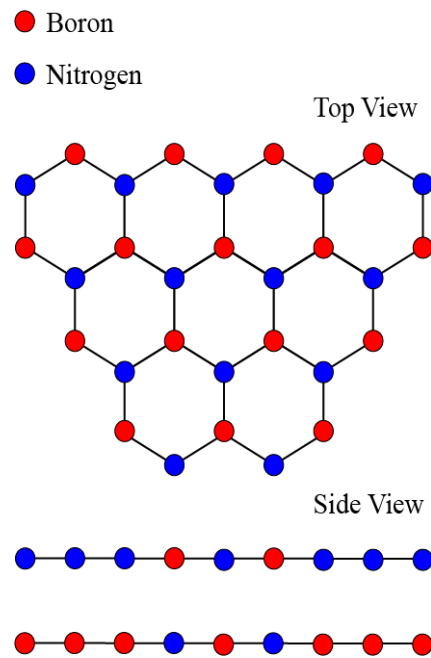
Figure 2-4: h-BN structure [35]

2.3.2   Properties and Applications

Primarily, boron nitride was considered as natural material, but after its discovery as reported in nature (journal), it can be made by experimentation [30]. The boron nitride nanosheets can be prepared by various techniques which will be discussed below. The h-BNNSs exhibit remarkable properties such as high temperature stability, high melting point, due to high electronegativity of nitrogen, it is electrically insulator with a band gap of 4-6 eV and white in color as compared to graphene which is electrical conductor and black in color. Due to its unique and unusual properties, h-BNNSs are used as reinforcing material for polymeric and ceramic nanocomposites. The out of plane weak bonding of BN makes it excellent industrial lubricants. The h-BNNS have found their use in medical field as of their good biocompatibility as they are also used in anticancer drug delivery due to high biocompatibility [31].

The experimental work on the single layer of h-BN for mechanical properties has not done yet, but stability of h-BN (in-plane) can be utilized for mechanical reinforcements. The theoretically predicted values for h-BN modulus and ultimate tensile strength (UTS) is around 720-950 GPa and 85 GPa respectively [37].

Due to these extraordinary properties, it can be used for the reinforcements of polymer to prepare nanocomposites. As both graphene and h-BNNS are similar in structure but their electrical properties are quite opposite. The graphene is electrical conductor while h-BNNSs is electrical insulator. Being excellent electrical insulator, it is excellent thermal conductor, the thermal conductivity range of h-BN nanosheets is 300-2000 W m^{-1} K^{-1}. This make h-BN nanosheets exceptional candidate for high power electronics in thermal management [38]. The wide band gap of h-BN can find its applications as a dielectric and insulting material between the layers of graphene. It also gains potential in using h-BN nanosheets as graphene's substrate [39].

Initially BN was considered as synthetic, but recently reported its discovery in nature [4], hexagonal boron nitride sheets (BNNSs) can be prepared by adopting several techniques including liquid phase exfoliation and wet rotating disc milling recently reported [17-18]. BNNSs have excellent electrical and mechanical properties due to unusual structural features.

2.4   Preparation of h-BNNS

The preparation of nanosheets using h-BN as a precursor in large quantities is utmost challenge. To make it cost effective and easily processed, the scientists discovered various production methods for h-BN nanosheets. The most commonly used lab scale fabrications of h-BNNSs are shown in figure 2-5.

Mechanical Exfoliation	Sonication assisted Exfoliation	Chemical Functionalized assisted Exfoliation
• Scotch tape cleavage • Ball milling • Blender shearing	• Exfoliation in organic solvents • Exfoliation in water • Exfoliation in acid	• Noncovalent functionalization • Covalent functionalization

Figure 2-5: Preparation methods of h-BN nanosheets [6]

2.4.1 Sonication Assisted Exfoliation

Sonication assisted exfoliation is essentially a method to separate the layers of h-BN to form BNNSs in various polar solvent using high energy ultrasonication which has the same surface energy as h-BN. Monolayered boron nitride as well as few layered boron nitrides have been obtained using this method. Without use of any advance equipment, this strategy is easy and scalable [13].

The most suitable method for applications where massive yield at low cost is required is sonication assisted exfoliation or delamination. This process is suitable for those materials in which layered structure is present as in graphite, these layers are stacked via van der Waals forces. This method can create high quality, high yield and defect free nanosheets. It can simply increase the accessibility of a material's surface area via sonication assisted exfoliation. Due to minimal flaws and defects the mechanical and thermal characteristics of nanosheets are well-preserved. Stankovich *et al* prepare monolayer graphene nanosheets using sonication assisted exfoliation in 2006 [40].

Coleman group was successful in producing single layer of graphene by exfoliation in liquid medium. Then they tried to exfoliate other material to prepare 2D nanosheets. They developed various system for 2D materials like h-BN, MoS_2, WS_2 etc. and developed suitable solvents and surfactants [41]. Hernandez *et al* and Zhi *et al* fabricated h-BN nanosheets using DMF as solvent to overcome the forces between the h-BN layers. Wang *et al* utilized acid such as methane sulfonic acid to exfoliate h-BN using sonication assisted exfoliation [42, 43].

2.4.1.1 Liquid Phase Exfoliation

This technique is all about applying different forms of energy to provide excitation in the solvent. In our work ultrasonication energy was used to excite h-BN. The ultrasonication energy overcomes the van der Waals forces of attraction between the h-BN layers in the solvent. The solvent can be any liquid chemical, aqueous or organic media. There are to main processes:

- Dispersion with ultrasonication
- Ultracentrifugation followed by vacuum filtration

Dispersion with ultrasonication

For liquid exfoliation the main requirement is to make a dispersion in a proper solvent. To make the dispersion compatible the solvent energy and attraction force between

layers of boron nitride to balance out. So that after exfoliation the sheets don't aggregate. The thermodynamics and energetics of systems should be well understood to find the best solvent for liquid exfoliation [44]. The mixing of two substances will change the enthalpy and entropy of system and enthalpy is the total energy of the system and entropy is disorder in the system. For the mixture to be favorable, the following thermodynamics relation needs to be followed:

$$\Delta G_{mix} = \Delta H_{mix} - T\Delta S_{mix}$$

$$\therefore \Delta G_{mix} \leq 0$$

During mixing, the entropy increases. For this to work, ΔS_{mix} needs to be positive. As for 2D materials ΔS_{mix} is very small. So, ΔH_{mix} play significant role. For ΔG_{mix} to be less than or equal to zero ΔH_{mix} needs to be very small. When scientist exfoliated graphene, they find different approximation for solvents to work with 2D sheets. Coleman group derived relation of ΔH_{mix} with surface energy of nanosheets and solvents [45]. Hilderband solubility parameters were formed to find the suitable solvent for dispersions [46]. To minimize the interfacial tensions between h-BN and solvent, the surface tension should be around 40 mJ m^{-2}. The solvents which can work best for dispersions of h-BN are isopropyl alcohol (IPA), dimethylformamide (DMF), benzyl benzoate, n-methyl-2-pyrrolidone (NMP), etc. [46]. The disadvantages of some solvents are high boiling point and toxicity. The surface tension for water is around 72 mJ m^{-2}. So, water cannot be used. Some researchers tried to find alternatives to use water as a solvent as it is less toxic. For this, they use surfactants to minimize the surface tension for liquid exfoliation [47].

After the selection of suitable solvent, sonic energy is provided to the dispersion. The whole setup is placed in an ice bath. The pressure changes as sonic energy frequency is >15 Hz which caused cavities to be formed in the dispersion. These cavities grow and collapsed as the shockwave propagate, shown in figure 2-6.

These cavities formation and their collapse play an important in exfoliation of these 2D sheets. When these cavities collapsed, the microjets near the surface. The microjets have enough energy to overwhelm the van der Waal forces present between layers. The speed of these microjets separates the layers to few-layers and monolayers. In a different scenario these cavities do not collapse and rebound from the surface to form a spherical nature and resulting in shockwaves to speed up and erode the material.
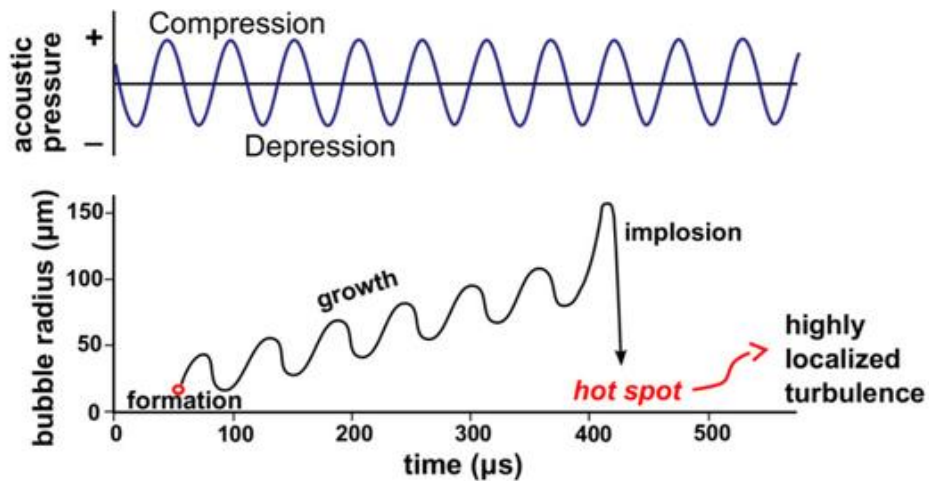
Figure 2-6: Schematic diagram of the ultrasonication in exfoliation process [48]

In addition to cavity formation by shockwave, another parameter that is also in effect is the inter planer collision of two-dimensional material. It produces another type of shockwaves that are more speedup. All these processes happening at the same time results in exfoliation of these 2D materials with different sizes and morphologies. It is also proven that the proper solvent will hold these nanosheets separated for longer time as compare to poor solvents which results in aggregation of the exfoliated sheets.
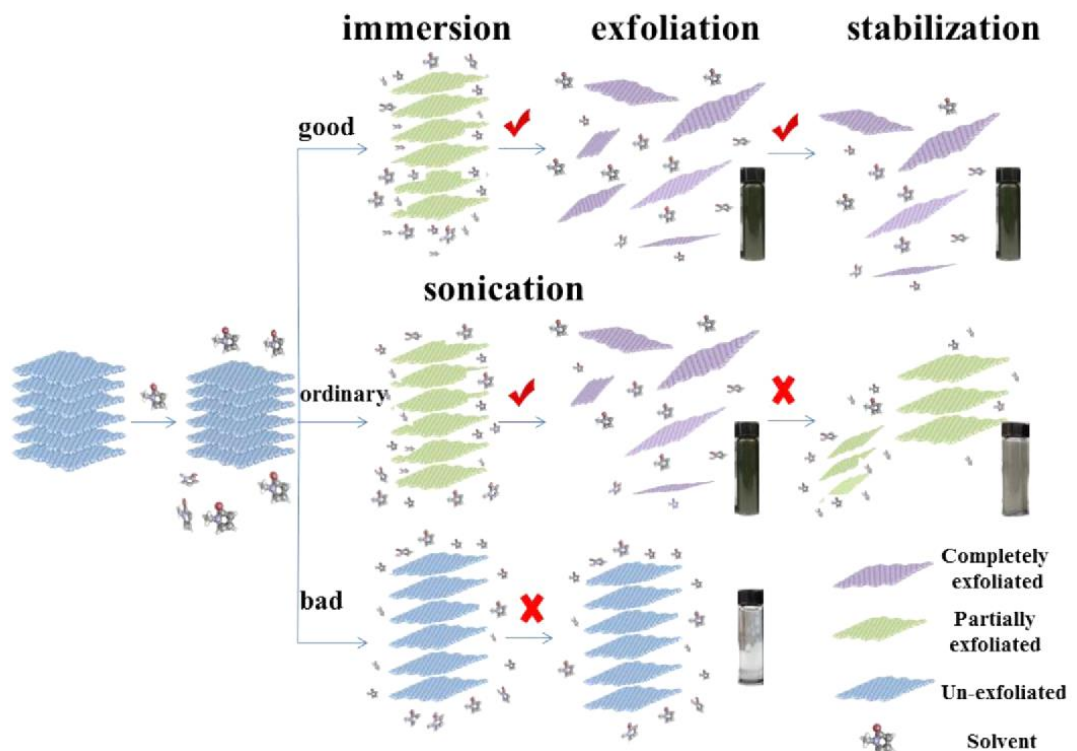
Figure 2-7: Sonication assisted exfoliation [49]

Ultracentrifugation followed by vacuum filtration

Ultracentrifugation is a process use to obtain same dimension of exfoliated sheets [50]. It is based on the centrifugation speed. At a fixed speed of ultracentrifugation, the heavier and unexfoliated sheets will settle down while lighter sheets will be suspended into the solvent. It is reported that using different centrifugation speeds, different sized nanosheets can be obtained. In the whole process, the ultracentrifugation at first started at higher speed (rpm). The supernatant is collected, and resultant sediment is mixed with solvent with sonication and then centrifuged at relative lower speed (rpm). Then the whole process is repeated and to obtain various sized nanosheets. It is also stated that higher the centrifuge speed, smaller the nanosheet length. The figure below shows the complete process.
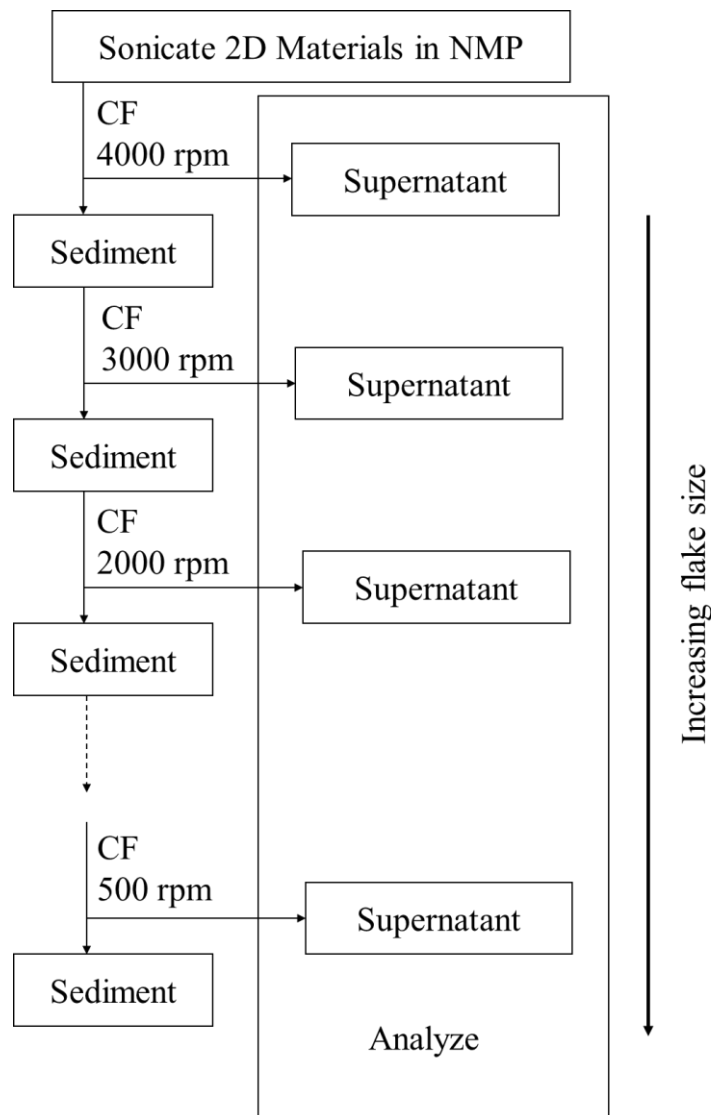
Figure 2-8: Ultracentrifugation process for 2D nanosheets [50]

After the ultracentrifugation, the supernatant is filtered out using membrane filters of 0.2-0.45 µm pore size for the removal of solvent. Vacuum filtration can also be used to speed up the process. The efficiency of these nanosheets depends on three factors [51-54]:

- Nanosheet dimensions
- Nanosheet thickness (no. of layers in each sheet)
- Quality of nanosheet

2.4.2 Mechanical Exfoliation

Novoselov *et al* prepared few layered graphene including monolayer by mechanical exfoliation (scotch tape method) of pyrolytic graphite in 2004 [55]. Pacile *et al* prepared BNNSs using micromechanical cleavage technique in which BN layers were separated using adhesive tape mounted on SiO_2 substrate [56]. Lee *et al* did comparative study using peeled off technique (mechanical cleavage) on Graphene, h-BN, $NbSe_2$ and MoS_2 to obtain their thin sheets [57]. The main drawback of micromechanical cleavage is that of low yield. So, a different technique i.e., ball milling was utilized to obtain nanosheets. Li *et al* prepare h-BNNSs using low energy ball milling to separates the layers of h-BN. The steel balls were used to apply shear forces to exfoliate h-BN layers [58].

2.4.3 Chemical Functionalization assisted Exfoliation

Chemical functionalization is an effective method for the exfoliation of laminated materials such as graphite, h-BN, CNTs etc. as chemical functionalization results in overcoming the van der Waal forces present between the layers or entities that binds these materials. Chemical functionalization is further divided into two parts:

- Noncovalent (Lewis acid-base ionic) functionalization
- Covalent functionalization

2.4.3.1 Noncovalent Functionalization

The organic materials attached to the h-BN surface or sometimes between the layers when dispersed in solvent, the solvation force generated by these bulky groups overcomes the van der Waals forces present among the layers results in exfoliation of h-BN to h-BNNS.

Takuya *et al* synthesized h-BNNS using noncovalent super acid functionalization of h-BN under sonication for their use in highly thermal conductive and electrical

insulating nanocomposite [59]. Wang *et al* non-covalently functionalized h-BN using cationic polyacrylamide to incorporate in polycarbonate to enhance thermal conductivity [60]. Bhimanapati *et al* used acid mixture of sulfuric and phosphoric acid to functionalize the h-BN which subsequently induce the exfoliation in h-BN to produce mono and few layers h-BNNSs [61]. Coa *et al* prepared isopropyl alcohol solution to exfoliate h-BN. They demonstrated that the mechanism for this exfoliation is based on Lewis acid-base [62]. Chae *et al* prepared noncovalent functionalized BNNS-OH using bile-based surfactants using sonication assisted exfoliation in aqueous media i.e., deionized water [47].

Figure 2-9: Schematic diagram of noncovalent functionalized BNNS-OH [47]

2.4.3.2   Covalent Functionalization

In covalent functionalization the bonding force is greater than that of non-covalent functionalization of h-BNNSs as it shows higher physical properties. Keeping this in mind, Huang *et al* experimented that the Lewis acidic CO_2 makes weak interaction with BN due to deficiency of electrons on its surface. They functionalized BNNS with electron rich amino polymers such as polyethyleneimine to capture CO_2 [63]. Sainsbury *et al* covalently functionalized BNNSs using dibromocarbene for manipulation of band gap and their use in nanocomposite [64].   Toby *et al* functionalized exfoliated h-BNNS by nitrene addition and then their utilization in polycarbonate to enhance mechanical properties [65].

2.5   Objectives

In this work, hydroxylated sonication assisted exfoliated boron nitride nanosheets (h-BNNSs-OH) in the presence of bile-base surfactant are used to disperse in poly methylene methacrylate (PMMA), via solution mixing to prepared nanocomposites to

study thermal and mechanical properties of fabricated nanocomposite. Simultaneously, the SAE boron nitride nanosheets (h-BNNSs) were also used to fabricate nanocomposite with PMMA to compare the results obtained as well as with pure PMMA.

Chapter: 3

Experimental Methods

In this chapter, the materials used for nanocomposite preparation, preparation of BNNSs, functionalization of h-BN and casting of nanocomposites are discussed in detail.

3.1 Materials

- Poly (methyl methacrylate) from Sigma Aldrich
- Boron nitride powder from Saint Gobin h-BN
- Isopropanol (IPA) from Sigma Aldrich
- Sodium deoxy cholate (SDC) from Sigma Aldrich
- Toluene from DaeJung Korea
- De-Ionized Water
- Filter membrane (Nylon, pore size 0.45 um)

3.2 BNNSs Preparation

The boron nitride nanosheets were prepared by using sonicated assisted exfoliation. For this procedure, three grams of h-BN powder at 50 mg ml^{-1} concentration were added to Isopropyl alcohol (IPA). The mixture was sonicated for 48 h using a probe sonicator. The sonication was done in ice bath. To obtain nanosheets, the sonicated mixture was centrifuged at 500 rpm for 45 minutes to obtain nanosheets (supernatant) from unexfoliated h-BN (sediment). The resultant supernatant was filtered by Nylon membrane. The filtered nanosheets were dried at 60 °C in heating oven. The resultant powder of BNNSs obtained after drying was used in nanocomposites preparation.

3.3 Functionalized BNNSs Preparation

The functionalization of h-BN was done by using hydroxylated sonicated assisted exfoliation process. For this procedure, 1.2 grams of h-BN powder at 20 mg ml^{-1} were added to de-ionized water (DI-water). 0.5 g of sodium deoxy cholate (SDC) was also added to the mixture as a surfactant. The mixture was sonicated for 48 h in ice bath. The sonicated mixture was then centrifuged at 500 rpm for 45 min to obtain required functionalized h-BN nanosheets as a supernatant. The supernatant was filtered through membrane. The obtained functionalized nanosheets were dried overnight at 60 °C.
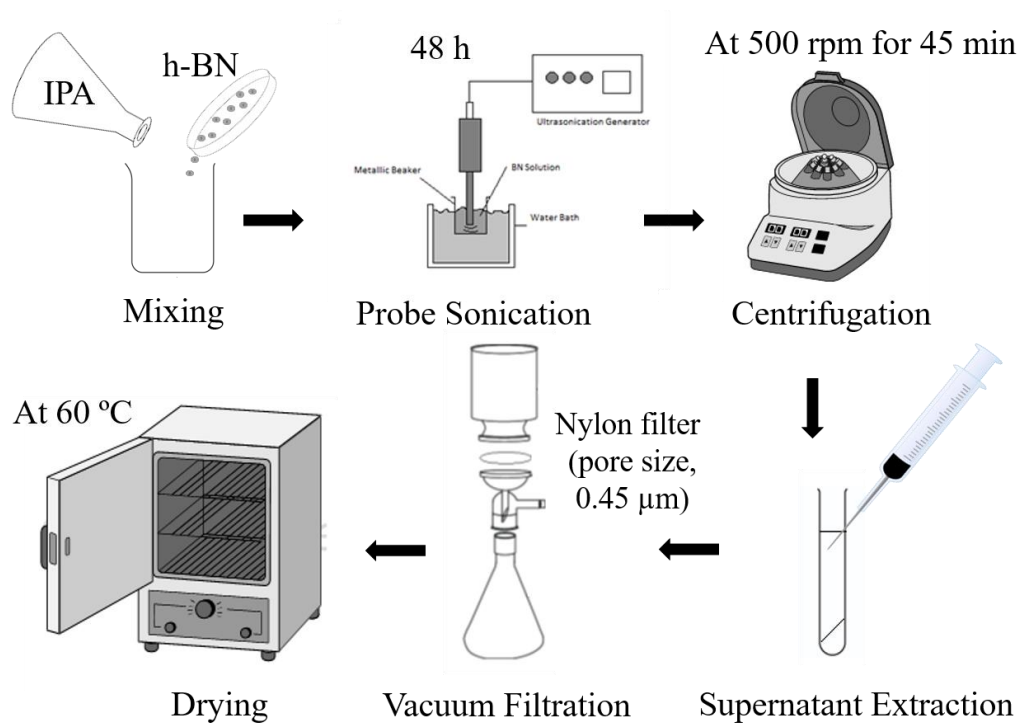
Figure 3-1: BNNSs Preparation
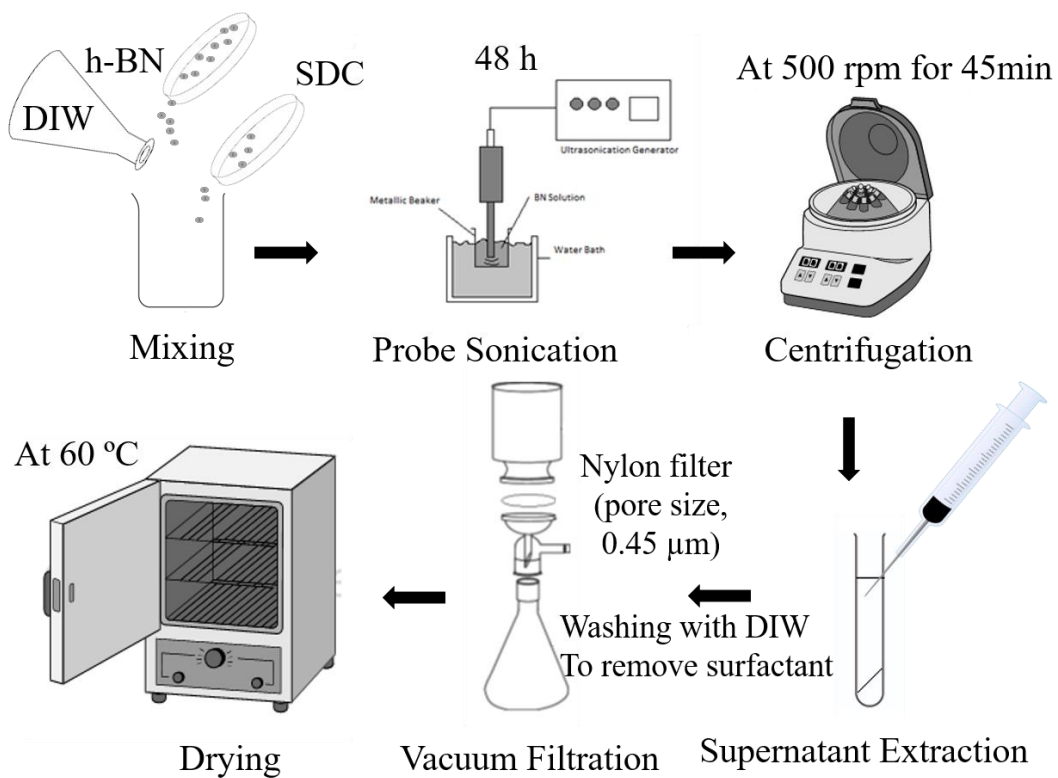
**Figure 3-2:** Functionalization of h-BN

3.4 Nanocomposite Preparation

Recent research shows that for nanocomposite fabrication, solution casting is well suited process which can be used to add h-BN nanosheets in numerous different polymers. Also, 2d nanosheets in suspensions are also attractive for utilization in solution casting process [66]. Thus, in this study solution casting was used to prepare nanocomposites.
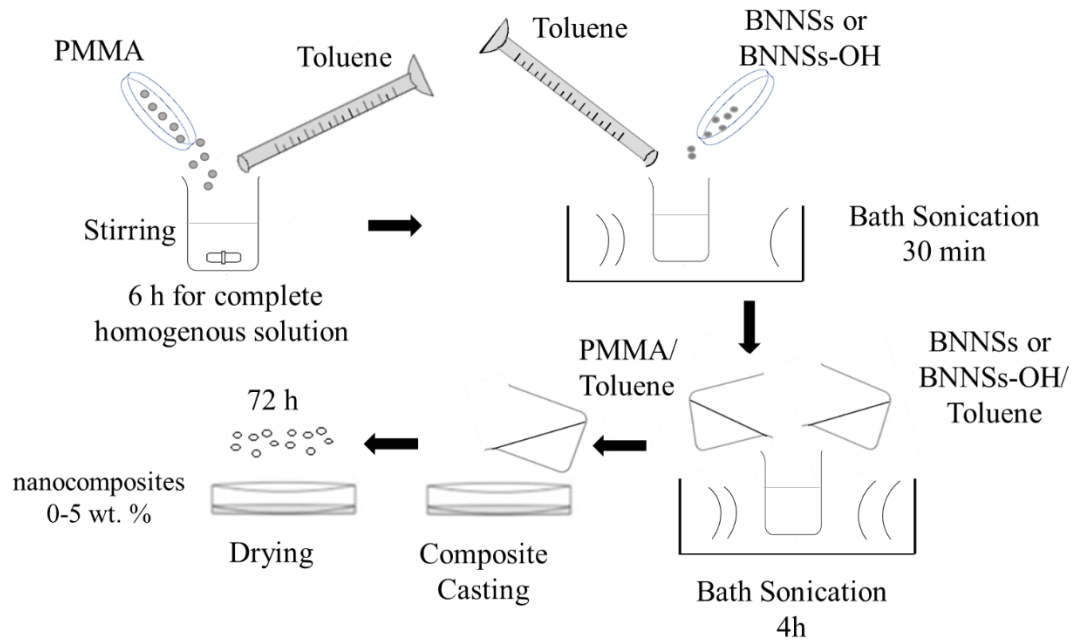
Figure 3-3: Preparation of nanocomposite

Pellets of PMMA, commercially known as plexiglass were obtained to prepare nanocomposites of PMMA/BNNSs and PMMA/BNNSs-OH, pellets of PMMA were dissolved in toluene at 120 mg ml^{-1} concentration and stirred for 6 h. BNNSs/Toluene and f-BNNSs/Toluene dispersions were prepared at a 5 mg ml^{-1} concentration. Various weight fractions (0-5 %) of BNNS-Toluene and BNNSs-OH were added to PMMA-Toluene to make nanocomposite dispersions. After 4 h of sonication in sonic bath, all the dispersed solutions were poured into glass petri dish and then dried for 72 h to naturally remove toluene (solvent) by evaporation. After the solvent removal, the free sanding films of nanocomposites were obtained and utilized for different characterization techniques and testing.

The table-1 showing the loading (wt. %) of BNNSs and BNNSs-OH in PMMA for nanocomposites

Table 1: Loading (wt. %) of BNNSs and BNNSs-OH in PMMA for nanocomposites fabrication

Sample No.	Loading (wt. %) BNNSs/BNNSs-OH in PMMA
1	0
2	0.1
3	0.5
4	1.5
5	2
6	5

Chapter: 4

Characterization Techniques

In this section, the different characterization techniques used are studied briefly.

4.1 X-ray Diffraction (XRD)

XRD is a structural characterization technique used to find the crystalline phase of sample and purity. This technique allows us to find the properties and structure at atomic level. It helps us to obtain bond length of atoms, how they are packed and in which crystalline structure, and their bond angle. It is also a non-destructive technique like scanning electron microscope. The XRD consists of the following parts:

- X-ray tube
- Monochromator (Collimator)
- Sample holder
- X-ray detector
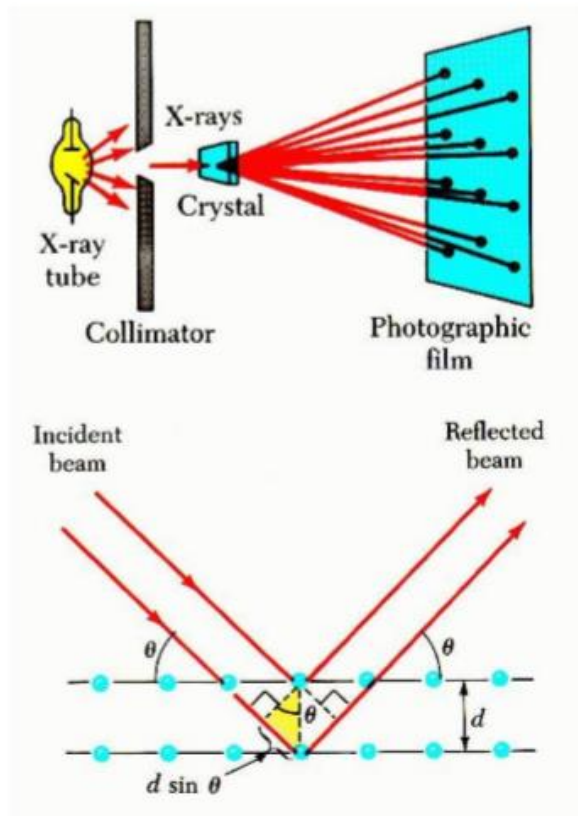
Figure 4-1: The basic schematic of XRD and Bragg's Law [67]

In this process, x-rays are produced by heating filament of cathode in x-ray tube. These x-rays are accelerated toward sample crystal after passing through monochromator. As sample crystal is made of atoms arrange to form regular planes. Some of the x-rays are absorbed and some of it having same wavelength as that of planes are reflected with the same angle of incident. That results in diffraction which is described by Bragg's law. The Bragg's law state that:

$$2 \, d \sin \theta = n \, \lambda$$

Here,

d = interplanar distance

θ = angle formed by crystal plane and incident beam

n = reflection order

The XRD works on Bragg's law, when constructive interference takes place, the law is satisfied. These Bragg's reflection gives the information about inter layer spacing, using this we can obtain unit cell dimensions, lattice mismatch and dislocations [67].

4.2 Scanning Electron Microscopy (SEM)

Scanning electron microscope (SEM) was performed to analyze sample structure and morphology. The beam of electron is fixated on the material's surface. The photons or electrons are knocked out from the material surface, these electrons and photons are directed toward the detector. The detector modulates he brightness of cathode ray tube. The points where electron beam focuses on the surface and interact with it results in a consequent point of cathode ray tube. That results in image formation. The SEM does not reveal the actual photo of sample surface, but actual image is shown electronically [68].

It is a non-destructive technique because it does no damage to sample after the electrons strike on the surface of material. The electron and surface interaction also result in secondary electrons, back scattered electrons and x-rays [69]. The common mode for SEM to obtain image is through secondary electrons, and the phase detection is via back scattered electrons. The basic information that can be obtained from SEM is:

- Morphology
- Topography

The components of SEM include:

- Electron column
- Specimen
- Secondary electron detector
- Back scattered electron detector
- Vacuum system
- Scanning system
- Electronic control
- Display

The schematic diagram of SEM is shown below,

The required analysis performed by SEM with following conditions:

- Sample is sputtered using gold
- Working distance of 10 mm
- 10-20 kV of operating voltage
- Current 90 mA
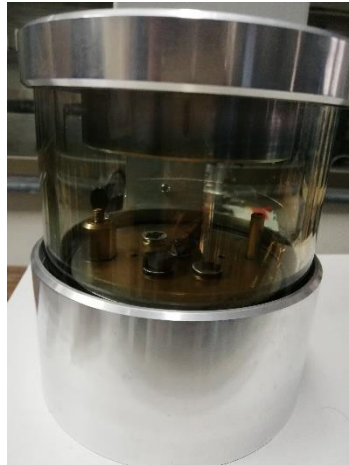
Figure 4-2: Sample preparation for SEM analysis using gold sputtering

4.3 Atomic Force Microscopy (AFM)

AFM is most valuable and versatile technique to study materials at nanometer scale. It is a type of scanning probe microscopes (SPMs). AFM uses force of attraction and repulsion to 3D image of sample. It is used to obtain aspect ratio and thickness of sample material. The image is obtained by the raster scan of AFM tip over the specified area of sample. In this technique the tip is attached to a cantilever [70].
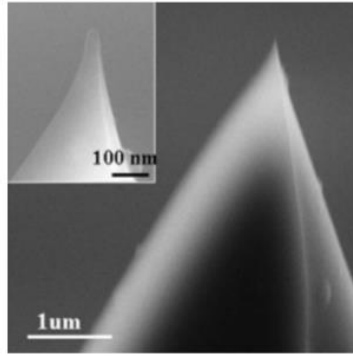
Figure 4-3: AFM tip [70]

As AFM works on the interatomic forces (van der Waals forces) during the raster scan, when tip reaches toward sample surface, tip deflects toward sample surface due to attractive forces and when it reaches near surface repulsive forces generated as both sample and tip come close together. This deflect the cantilever from the surface. The deflections of the cantilever are measured to acquire image resolution with AFM. The optical lever mirrored the laser towards the cantilever. The mirrored laser beam hits a detector comprising of four-section detector (photo). The changes in signals between the segments of photo-detector indicate angular deflections of the cantilever as shown in figure.

The AFM images was obtained by JOEL JSPM-5200. The samples were prepared by preparing a solution of BNNSs and BNNSs-OH in IPA and deionized water and then drop casted on glass slide and dried. The length, height and aspect ratios were studied using AFM images.
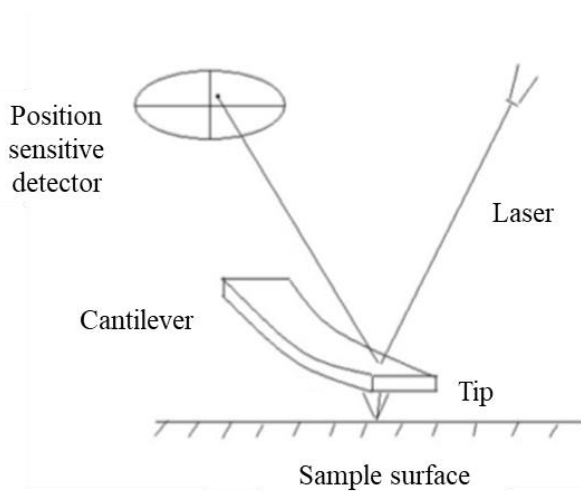
Figure 4-4: AFM working principle [70]

4.4 Fourier Transform Infrared (FTIR) Spectroscopy

The FTIR is an investigative technique to find functional groups in organic materials and sometimes inorganic materials as well. This method uses infrared radiation to fall on sample to observe its chemical properties. Every atom in a molecule above absolute temperature is in continuous vibration. So different functional groups absorbed IR radiations with respect to their characteristic frequencies. Using functional groups, we can identify different compounds [71].

In infrared spectroscopy, when IR radiations are directed on the sample, the frequency of vibration of a molecule in a sample when ties with the infrared radiation frequency, it absorbed that radiation. There are mainly two different vibrations:

- Stretching
- Bending

The IR spectroscopy uses interferometer to provide the resulting infrared spectrum. The interferometer as shown in figure 4-6, consists of three main parts:

- Source
- Detector
- Beam splitter

In this technique infrared light is directed toward the beam splitter present in the interferometer as shown in figure, the moving and mixed mirror reflect the infrared beams to beam splitter, these beams recombine constructively and destructively at beam splitter and directed towards the sample which is detected as an interferogram. This interferogram is converted into IR spectrum using Fourier Transform. The resulted spectrum is shown a light output (% transmittance) as a function of wavenumber [71].
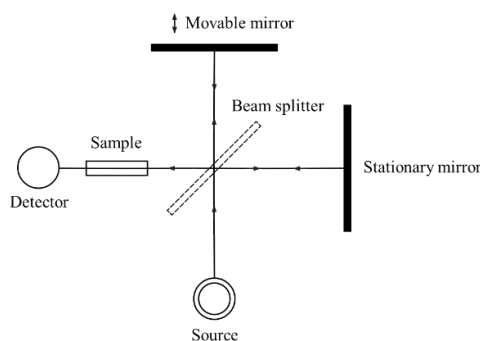

Figure 4-5: Schematic of interferometer [71]

4.5 Differential Scanning Calorimetry (DSC)

DSC is thermal investigation technique which measures heat flows and temperature related to thermal transitions in a polymer with respect to temperature and time. The nitrogen gas is used to provide inert environment during testing. Using this we can measure qualitative and quantitative data about chemical and physical changes involving changes in heat capacity or, exothermic and endothermic processes. Using DSC, we can measure melting points, T_g, crystallization temperature and time, % crystallinity and heat of fusion and reactions. In this technique, increase in temperature at both sample and reference pan is plotted against the amount of heat absorbed or released [72]. The DSC equipment consists of the following components:

- Sample and reference holder
- Heater
- Thermocouple
- Heat sink (chiller)
- Inert gas cylinder
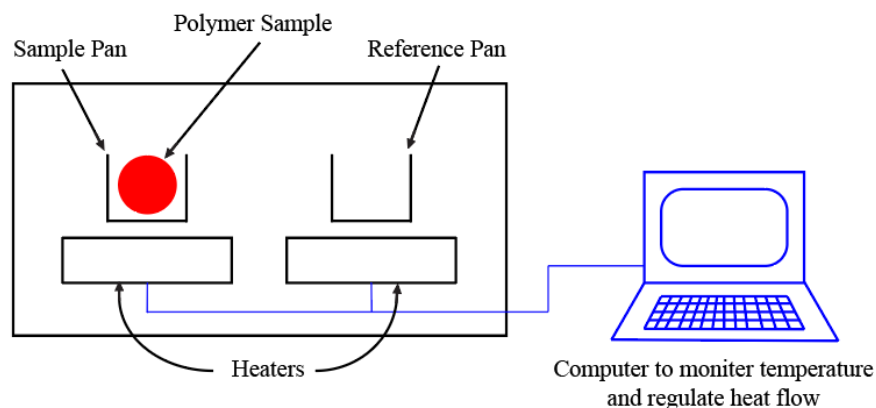
Figure 4-6: Schematic of DSC apparatus [72]

4.6 Mechanical Testing

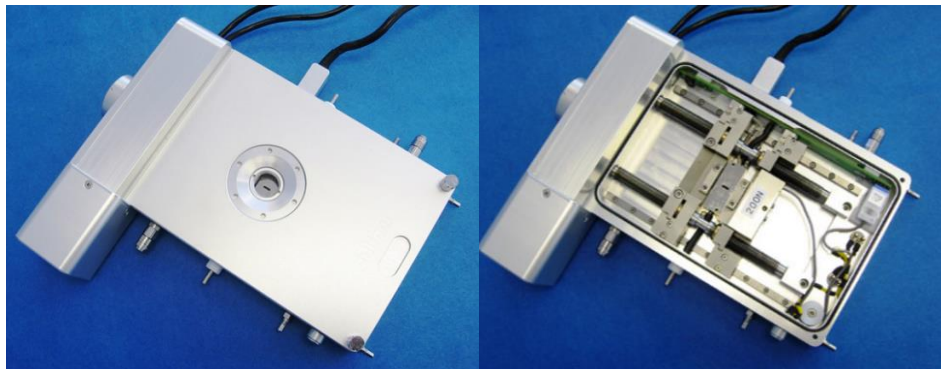Mechanical testing was done by tensile stress testing (TST). The equipment has two stainless steel jaws which move in opposite directions. The sample can be loaded into jaws very quickly and test can be performed in no time. The force transducer that is built in the equipment to display data plot online between force and distance relative to temperature. Using these plot data, we can obtain:

- Stress-strain curve

- Ultimate tensile strength

- Fracture point

- Strain at break

- % elongation

- Toughness

- Modulus of elasticity (Young's modulus)

The material to be tested is place inside the jaws of TST and an axial force is applied. The strain is produced and recorded until material reached its fracture point and breaks. The change in length is measured to obtain the stress-strain relationship. The following are the components of TST:

- Sample chamber

- Built in valves for gas inlet

- Engine

- Screws

- Gripping jaws

- Force transducer

- Specimen

Figure 4-7: Tensile stress testing system

Chapter: 5

Results and Discussion

This chapters will address the results and detail discussion of characterizations, thermal and mechanical (tensile) testing of fabricated nanocomposites.

5.1 Scanning Electron Microscopy (SEM)

The morphology of nanosheets was analyzed by SEM. Figure 5-1a and 5-1b shows the morphology of exfoliated BNNSs and functionalized BNNSs-OH respectively, which showed that the sheets are uniform and had polygonal shape and smooth surfaces. The average length/width of BNNSs and BNNSs-OH were 1.41/1.11 µm and 1.67/1.28 µm respectively.
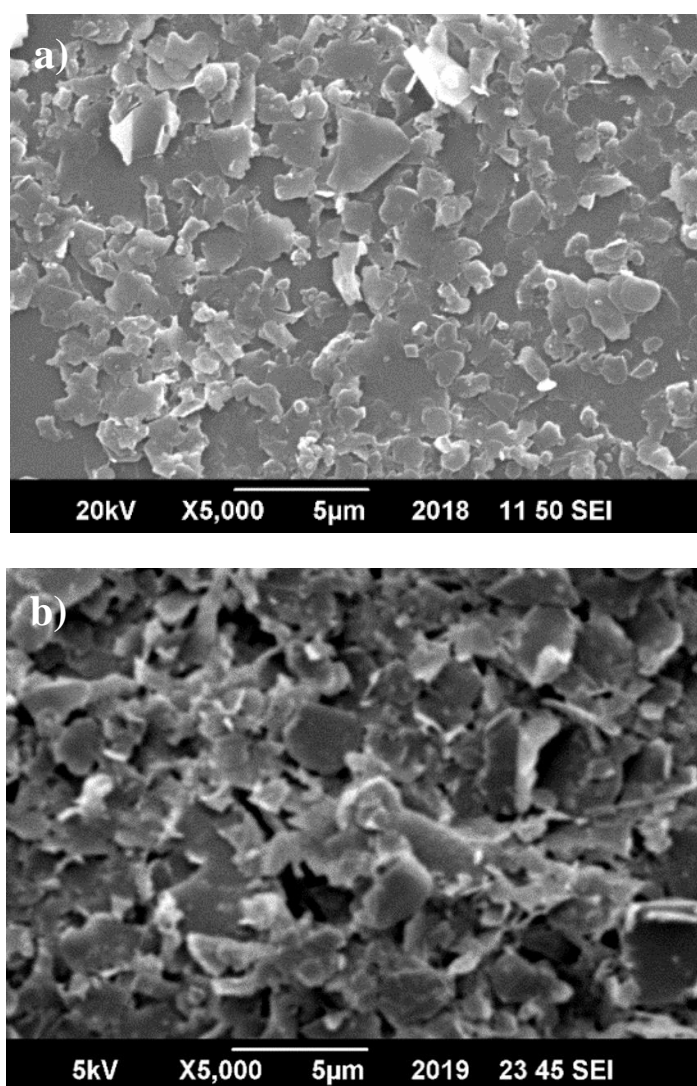
Figure 5-1: SEM images of a) cluster of BNNSs and b) cluster of functionalized BNNSs-OH

To study the dispersion of nanosheets and morphology of polymer nanocomposites, it is best to analyze SEM at cross-section for polymer nanocomposites. As shown in figure 5-2a, the pure PMMA film cross-section that showed the smooth surface that revealed the brittle fracture behavior [73]. SEM images also show that as the filler wt. % increases, the structure become distorted. The figure 5-2b and 5-2c shows that the poor dispersion of BNNSs resulted in agglomeration. The figure 5-2e and 5-2f show the better dispersion of 0.5 wt. % BNNSs-OH and 5 wt. % BNNSs-OH respectively as compared to non-functionalized BNNSs/PMMA nanocomposites. These images showed that the functionalization resulted in better dispersions of nanosheets.

a)

5kV   X3,000   5µm   2019   26 40 SEI

b)

10kV   X5,000   5µm   2019   19 42 SEI
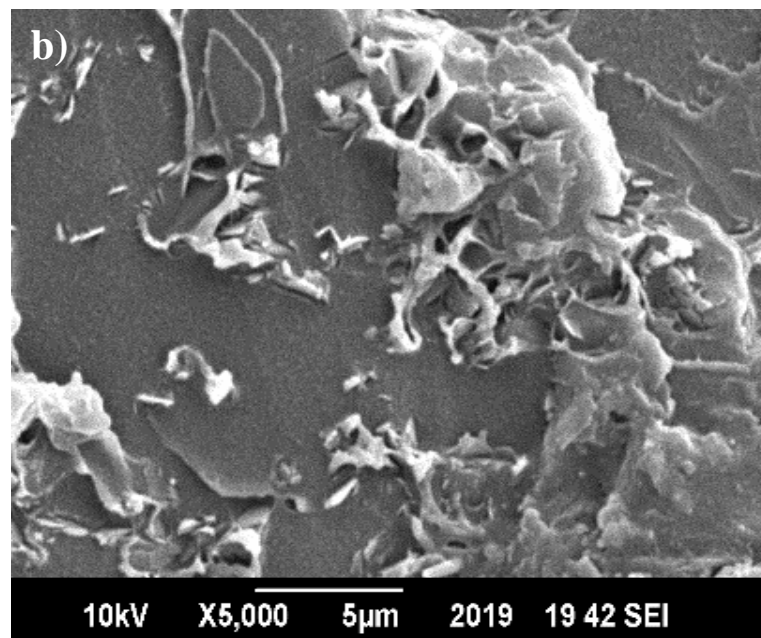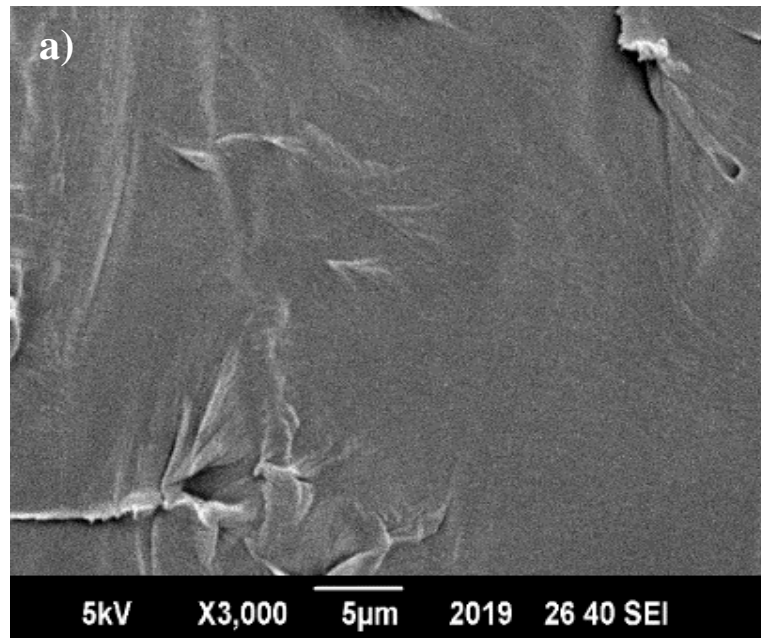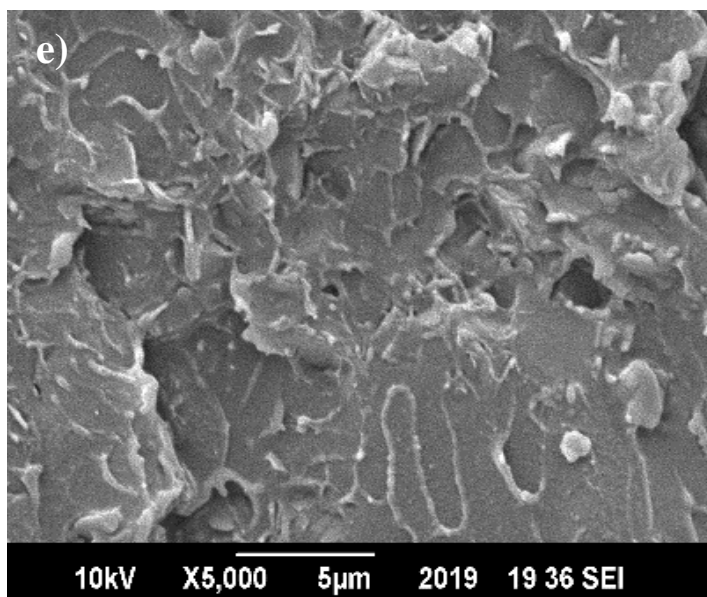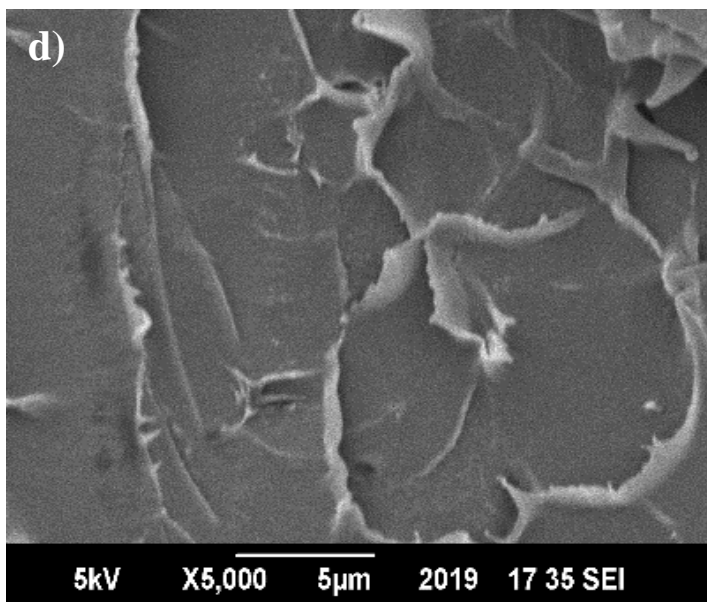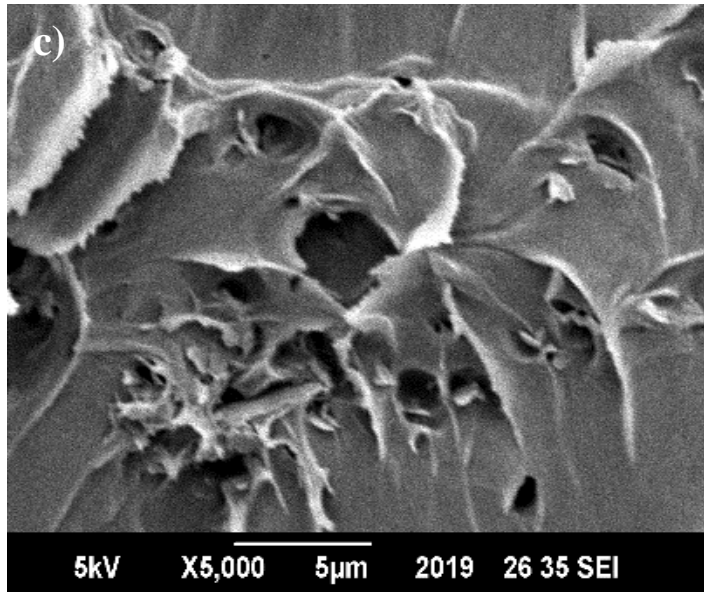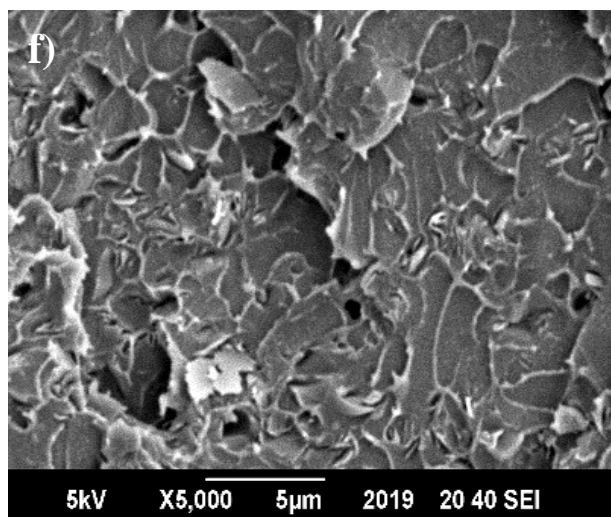
Figure 5-2: SEM images a) pure PMMA, b) 0.5 wt. % BNNSs, c) 2 wt. % BNNSs, d) 0.1 wt. BNNSs-OH e) 0.5 wt. % BNNSs-OH and f) 5 wt. % BNNSs-OH in PMMA nanocomposites

5.2 X-Ray Diffraction (XRD)

X-ray diffraction patterns for BNNSs and BNNSs-OH as shown in figure 5-3, indicating the strong peaks of (002) at $2\Theta = 26^{\circ}$, which exhibited that the BN structure is highly crystalline. XRD pattern also revealed the four small characteristics peaks of BN at $2\Theta = 41^{\circ}$, 43°, 50° and 54° corresponding to the planes of (100), (101), (102) and (004) respectively (JCPDS card no. 85-1068). The functionalized BNNSs also showing the similar pattern as of non-functionalized BNNSs which showed the crystal structure of BN was not disturbed after functionalization. As hydroxyl group attached to the edges of nanosheets which will not change the lattice spacing.
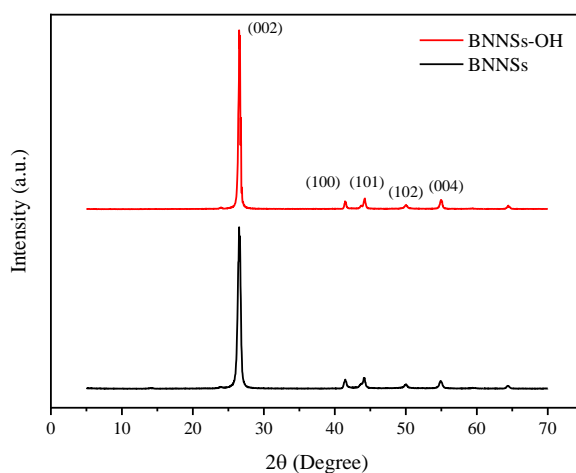
Figure 5-3: XRD patterns for BNNSs and BNNSs-OH

XRD pattern for Pure PMMA indicating amorphous nature of polymer [74] as shown by the broad peak at around $2\Theta = 19^\circ$. While XRD pattern for polymer nanocomposites showing peaks for BN at the same position ($2\Theta = 26^\circ$) as that of pure BN in figure 5-4. Also, the intensity of BN peaks increases with increasing BNNSs wt. %. The similar trend was followed by BNNSs-OH/PMMA XRD patterns as shown in figure 5-5. The broad peaks for PMMA in functionalized nanocomposites are also affected due to strong interaction of PMMA and BNNSs-OH.
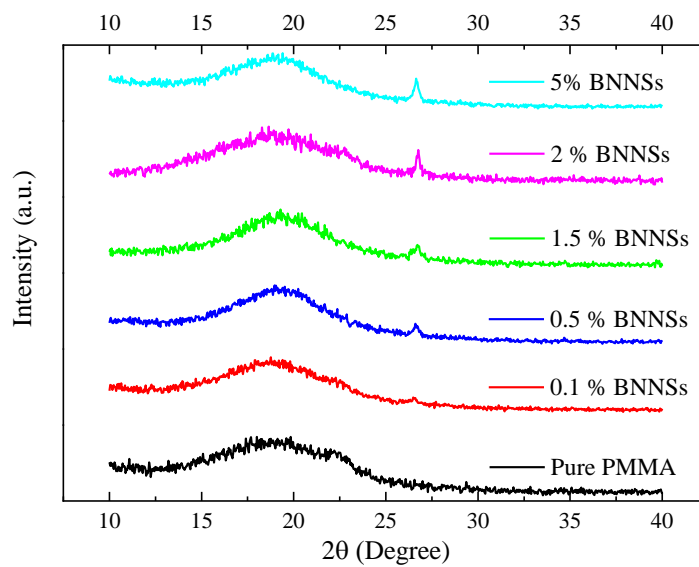
Figure 5-4: XRD Pattern of BNNSs/PMMA composites
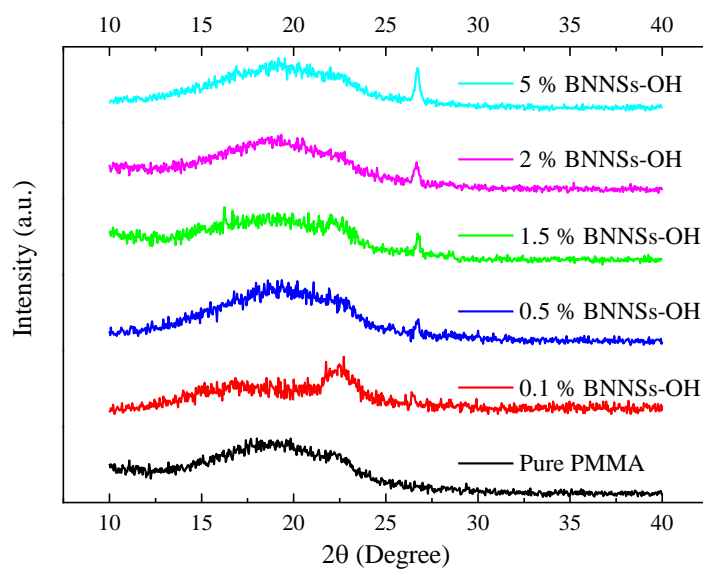
Figure 5-5: XRD Pattern of BNNSs-OH/PMMA composites

5.3 Atomic Force Microscopy (AFM)

In this study, the nanosheets which were extracted from the supernatant that was obtained at 500 rpm speed of centrifugation. To find the thickness of nanosheets, atomic force microscopy was studied. Figure 5-6 and 5-7 showing AFM images of BNNSs and BNNSs-OH. The histograms of AFM as shown in figure 5-8, shows that the most nanosheet flake thickness is around 10-25 nm. There are some flakes of <10 nm thickness. The functionalized BNNSs-OH histogram as shown in figure 5-9, showed the reduce thickness as most flakes thickness is around 1-10 nm. The aspect ratios for BNNSs and BNNSs-OH were ~94 and 336 respectively. This showed that the functional groups (OH) present at the edges of nanosheets help in exfoliation of nanosheets as OH groups repel each other.
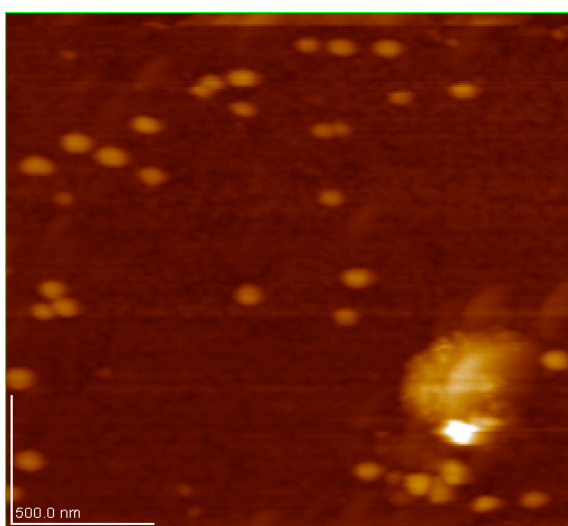
Figure 5-6: AFM image of BNNSs
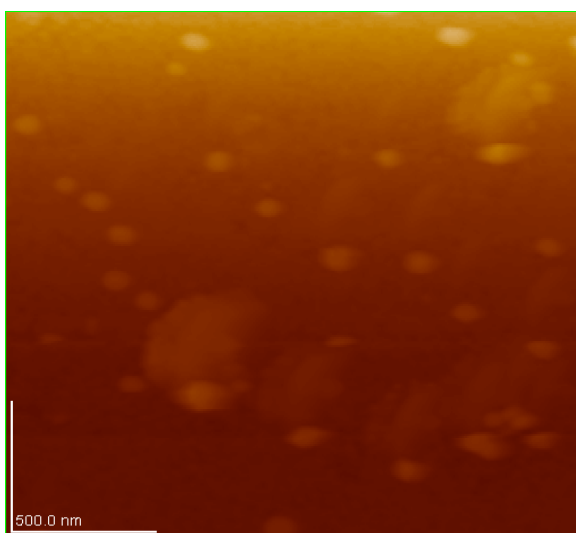
Figure 5-7: AFM image of BNNSs-OH

35
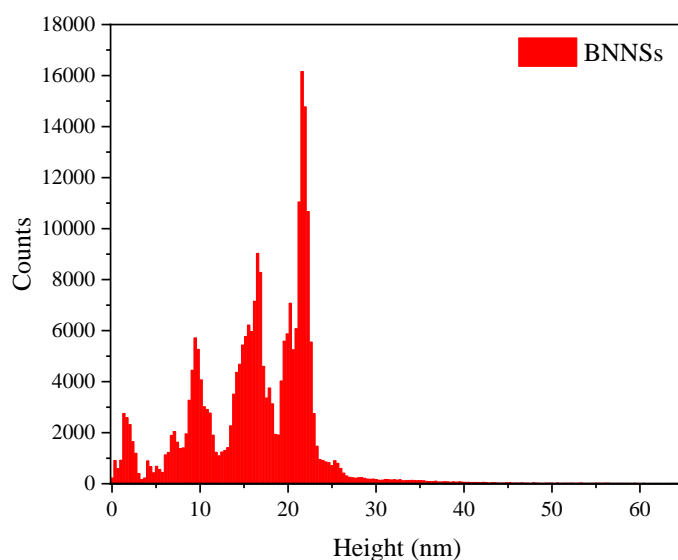
Figure 5-8: Histogram of BNNSs showing flakes thickness
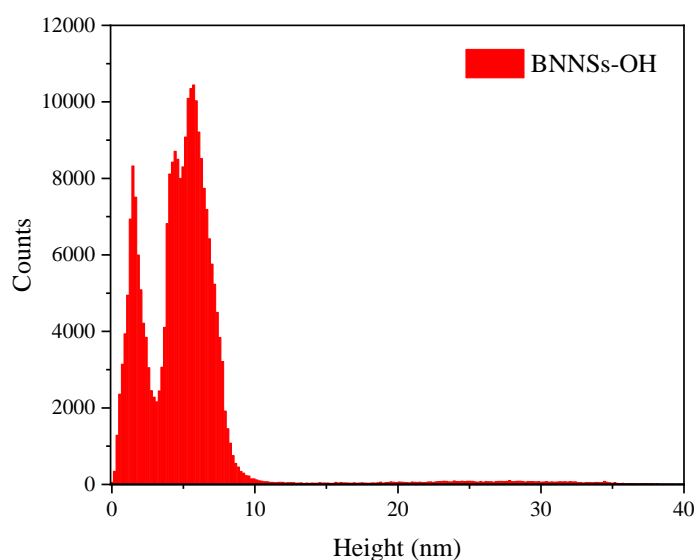
Figure 5-9: Histogram of BNNSs-OH showing flakes thickness

5.4 Fourier Transform Infrared (FTIR) Spectroscopy

FTIR analysis was performed to characterize the h-BNNS and OH-BNNS to confirm whether h-BNNS is functionalized with hydroxyl (-OH) group or not. As shown in figure 5-10, the broad peak at 3435 cm^{-1} exhibited stretching peak for O-H which was resulted from hydroxylated assisted sonication of h-BN in the presence of surfactant.

While two peaks at 1372 cm^{-1} and 816 cm^{-1} showed the in-plane stretching and out of plane bending for B-N bond.
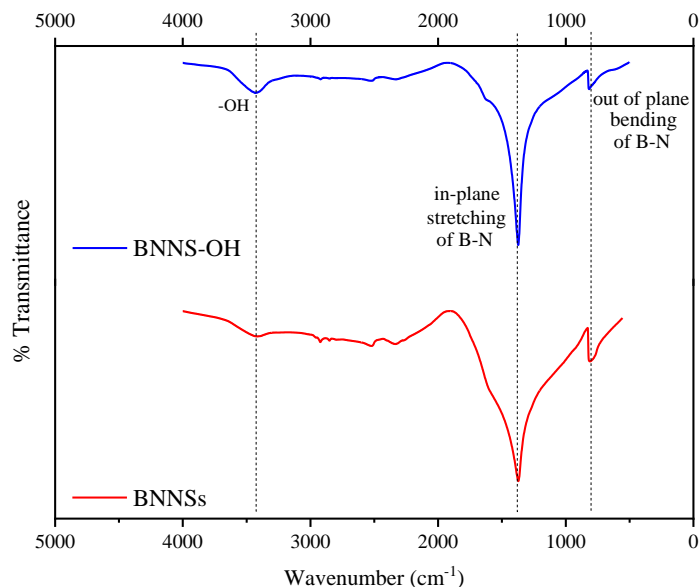
Figure 5-10: FTIR spectra of BNNSs and BNNSs-OH

As in figure 5-11, the peaks around 3000 cm^{-1} wavenumbers show the sp^3 C-H stretching present in polymeric chains of PMMA, the 1607 cm^{-1} wavenumber peak shows the stretching of C=O bond and 1180 cm^{-1} wavenumber peak shows stretching of C-O bond, confirming the functional groups of PMMA. By adding BNNSs and BNNSs-OH, the peaks of B-N bond were at around the same position as that of BNNSs and BNNSs-OH peaks as discussed above.
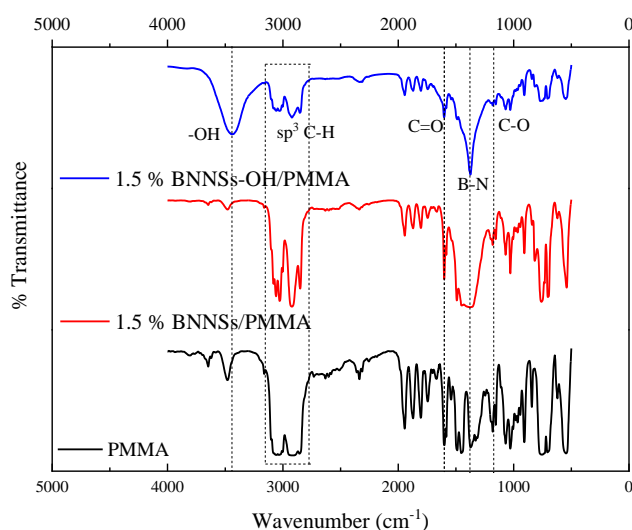
Figure 5-11: FTIR spectrum of pure PMMA and its nanocomposites with 1.5 wt. % BNNSs and 1.5 wt. % BNNSs-OH

The nanocomposite of BNNSs-OH/PMMA showed a broad peak of -OH (hydroxylic group) at 3439 cm^{-1} wavenumbers, which showed that the functional group of OH is present in the composite.

5.5   Differential Scanning Calorimetry (DSC)

Differential scanning calorimetry (DSC) results shows that T_g (glass transition temperature, the temperature above which polymer shows rubbery behavior and above which it shows glassy behavior) for PMMA in the beads form (as received bulk PMMA) is around 107 ℃. After making thin films of PMMA using toluene as a solvent the T_g decreases to 86.5 ℃ for pure PMMA films as shown in figure 5-12, this is due to number of reasons. The first is related to structure of bulk polymer is affected by the addition of solvent and polymer molecules interaction. The second, it may be due to the retention of solvent during drying process. The third, addition of solvent may distort the polymer chains which resulted in reduced T_g [75].
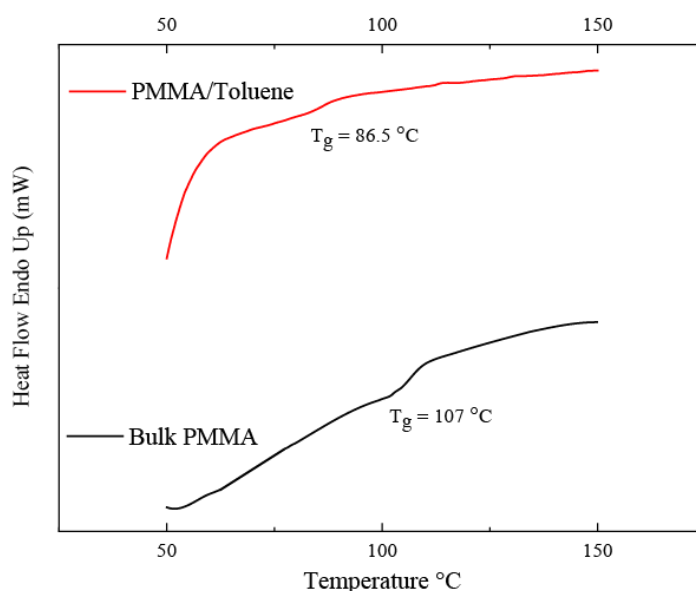
Figure 5-12: DSC curves of Bulk PMMA and PMMA/Toluene

The figure 5-13 shows that the glass transition temperature of BNNSs/PMMA nanocomposites decreases with the increase in wt. % of BNNSs. BNNSs showed the phenomena of "intercalation", thus creating free space between chains, enhancing the mobility of chains [76]. This results in polymer needing less energy, lowering the glass transition temperature. As the concentration increases to 5 wt. %, the T_g reduced to 69.37 ℃, which can be due to agglomeration at high concentration tend to increase more spaces between chains results in further decrease in glass transition temperature.

The similar trend can be found for BNNSs-OH/PMMA nanocomposite glass transition temperature in figure 5-14. But it is less pronounced as compared to non-functionalized (BNNSs/PMMA) nanocomposite. This showed that the due to strong interaction between functionalized BNNSs-OH and PMMA, the T_g increased as compared with non-functionalized BNNSs. This results in better dispersion due to functionalization of h-BN. Table-2 showing glass transition temperatures of as prepared nanocomposites.
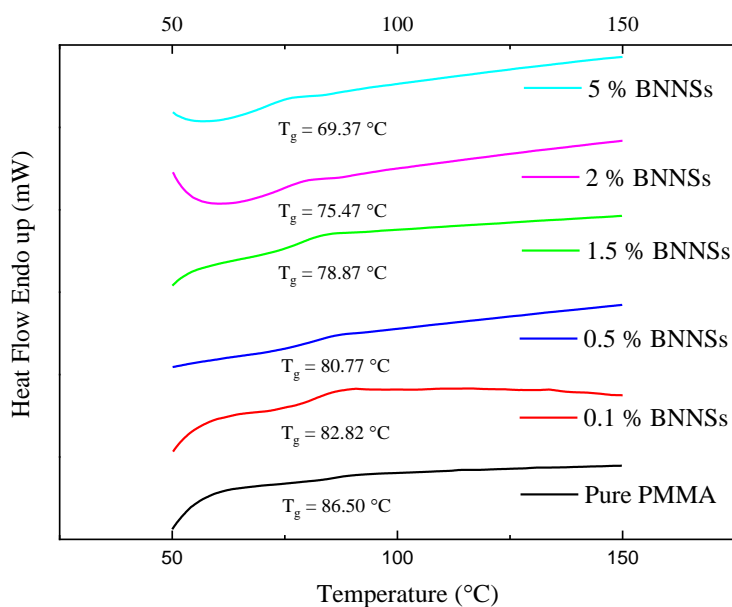
Figure 5-13: DSC curves of PMMA nanocomposite with BNNSs
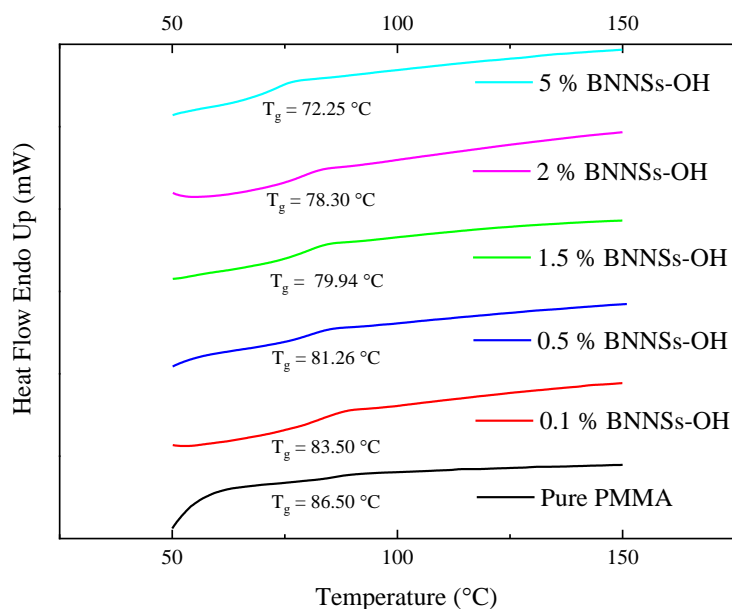
Figure 5-14: DSC curves of PMMA nanocomposite with BNNSs-OH

Table 2: Glass transition temperature of BNNSs/PMMA and BNNS-OH/PMMA nanocomposites

Loading, wt. % of BNNSs/BNNSs-OH	Glass Transition Temperature (ºC) of BNNSs/PMMA	Glass Transition Temperature (ºC) of BNNSs-OH/PMMA
Blank PMMA	86.50	86.50
0.1	82.82	83.50
0.5	80.77	81.26
1.5	78.87	79.97
2	75.47	78.30
5	69.37	72.25

5.6 Mechanical Testing

The mechanical testing was performed in tensile (tension) mode using Tensile Testing system. The samples were cut according to ASTM standard in a rectangular strip (20 mm gauge length, 10 mm width) with a strain rate of 1 mm/min, to obtain stress-strain graphs, as shown in figures 5-15 and 5-16 for BNNSs/PMMA and BNNSs-OH nanocomposites.
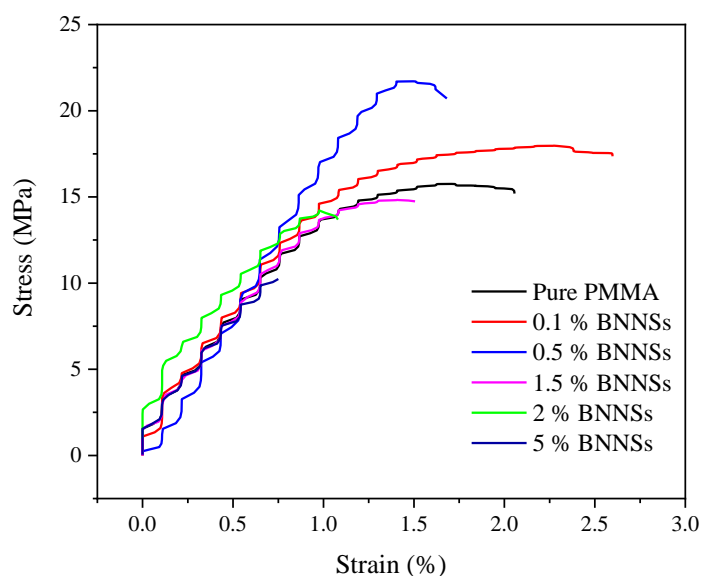
Figure 5-15: Stress-strain curves for BNNSs/PMMA nanocomposites
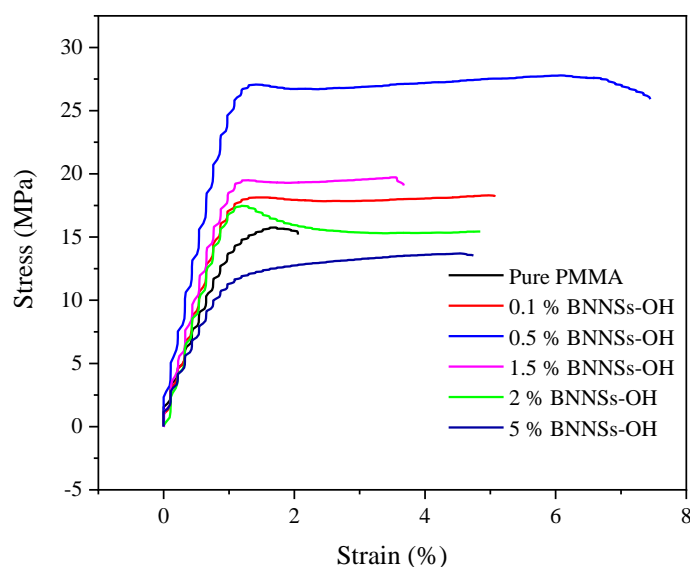
Figure 5-16: Stress-strain curves for BNNSs-OH/PMMA nanocomposites

Tensile strength of BNNSs/PMMA nanocomposite as shown in figure 5-17 increases up to 1.5 wt. % BNNSs as compared to pure PMMA (15.05 MPa) and maximizes at 0.5 wt. % BNNSs ~19.68 MPa. This is due to profound interaction between PMMA and BNNSs as mechanical load is transferring to BNNSs. But at high loading (2-5 wt. %) the tensile strength decreases drastically due to agglomeration, so load cannot be transferred effectively and due to increase concentration of defects related to BN sheets embedment. The similar trend is followed for functionalized nanocomposites (BNNSs-OH/PMMA) as shown in figure 5-18. The maximum tensile strength is achieved at 0.5 wt. % BNNSs-OH ~ 25.99 MPa with an increase of 72.69 %. This increase is due to better uniformity obtained by functionalizing BNNSs with OH group to enhance the interaction of BNNSs with PMMA molecules. Table-3 showing tensile strength of prepared nanocomposites.

Table 3: Tensile strength of BNNSs/PMMA and BNNSs-OH nanocomposites

Loading (wt. %)	Tensile Strength (MPa) of BNNSs/PMMA	Tensile Strength (MPa) of BNNSs-OH/PMMA
Blank PMMA	15.05	15.05
0.1	16.14	17.13
0.5	19.68	25.99
1.5	16.27	19.19

| 2 | 13.97 | 16.04 |
| 5 | 10.15 | 11.13 |
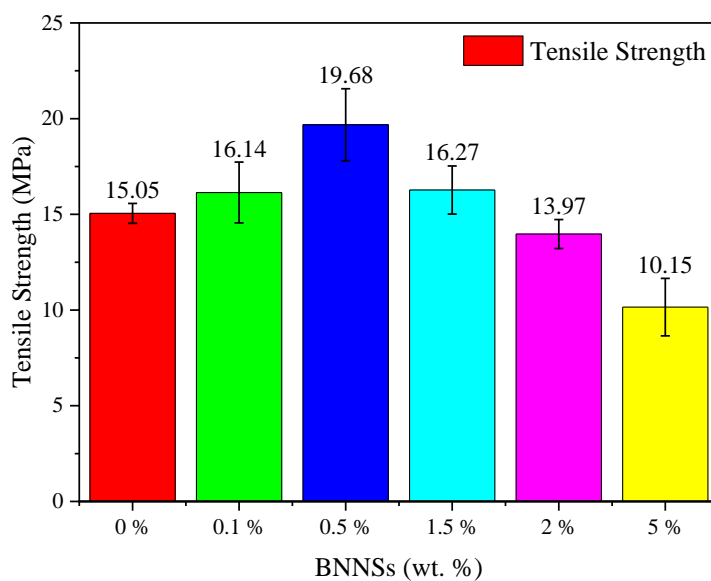
Figure 5-17: Tensile strength of PMMA and its nanocomposites with BNNSs at different loading (wt. %)
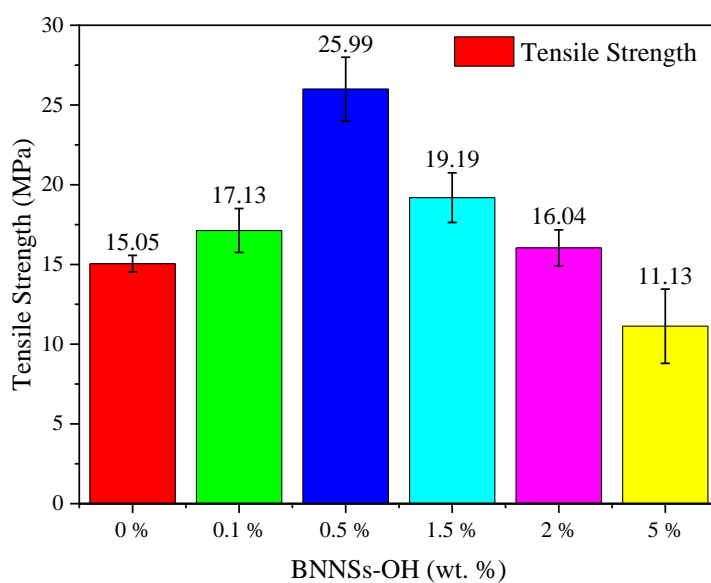
Figure 5-18: Tensile strength of PMMA and its nanocomposites with BNNSs-OH at different loading (wt. %)

Young's Modulus of BNNSs/PMMA nanocomposite as shown in figure 5-19, increases up to 2 wt. % BNNSs (2.03 GPa) as compared to pure PMMA (1.45 GPa),

at higher concentration (5 wt. %) it decreases. There may be dispersion issues and aggregation of BNNSs in PMMA. For functionalized BNNSs-OH/PMMA nanocomposites, shown in figure 5-20, the young's modulus peaking at 0.5 wt. % BNNSs-OH/PMMA, 2.19 GPa. Interestingly, the tensile strength of functionalized BNNSs-OH nanocomposite also maximizing at 0.5 wt. % of BNNSs-OH. After that it is decreasing as structure is distorting due to addition of nanosheets. The table-4 showing Young's modulus of prepared nanocomposites.

Table 4: Young's modulus of BNNSs/PMMA and BNNSs-OH nanocomposites

Loading (wt. %)	Young's Modulus (GPa) of BNNSs/PMMA	Tensile Strength (GPa) of BNNSs-OH/PMMA
Blank PMMA	1.45	1.45
0.1	1.42	1.52
0.5	1.51	2.19
1.5	1.83	1.77
2	2.03	1.34
5	1.61	1.24
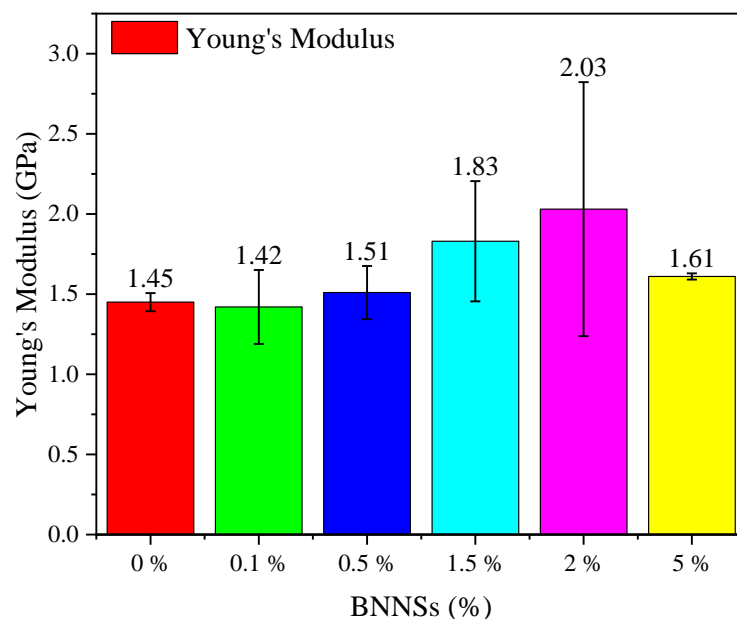
Figure 5-19: Young's modulus of PMMA and its nanocomposites with BNNSs at different loading (wt. %)
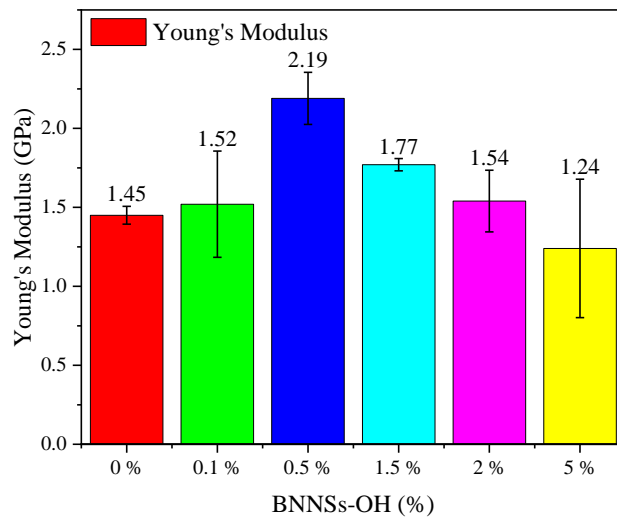
Figure 5-20: Young's modulus of PMMA and its nanocomposites with BNNSs-OH
at different loading (wt. %)

The nanocomposites indicating the increase in % strain at break for non-functionalized
BNNSs, as shown in figure 5-21, peaking at 0.5 wt. % but after that it decreases below
the base polymer, which shows that the load is not transferring to nanosheets and
dispersion may also be an issue is it was evident by tensile strength and SEM cross-
sectional images of non-functionalized BNNSs-PMMA nanocomposites. But after
functionalization as shown in figure 5-22, the % strain at break increases drastically
because of better dispersion and it is evident that nanocomposites are getting tougher.
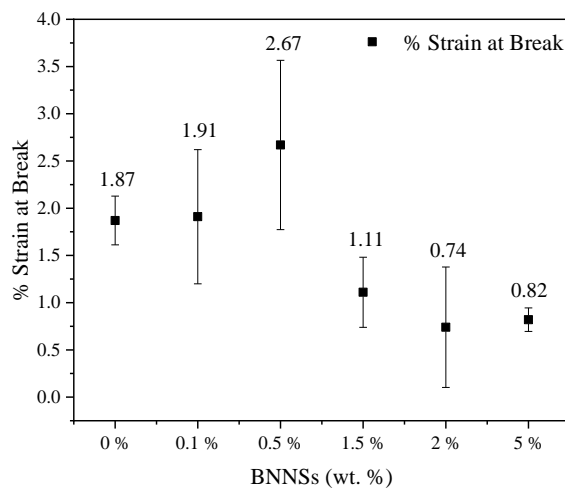
Figure 5-21: % strain at break for PMMA and its nanocomposites with BNNSs at
different loading (wt. %)
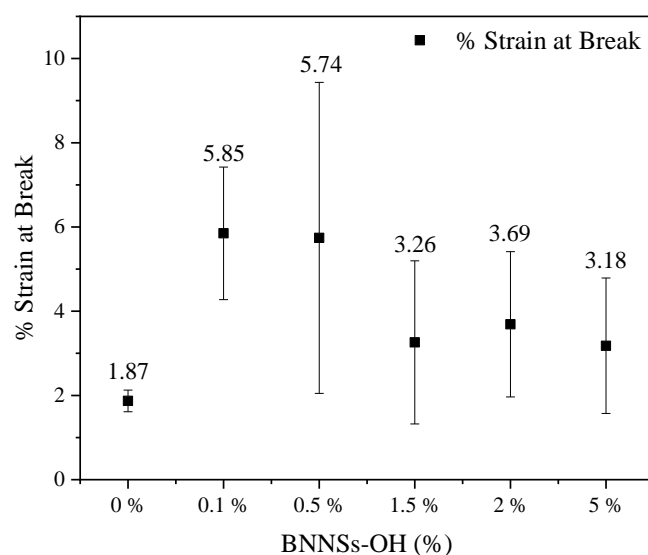
Figure 5-22: % strain at break for PMMA and its nanocomposites with BNNSs-OH at different loading (wt. %)

The Table-3 showing % strain at break of prepared nanocomposites.

Table 5: Strain at break of BNNSs/PMMA and BNNSs-OH nanocomposite

Loading (wt. %)	Strain at Break (%) of BNNSs/PMMA	Strain at Break (%) of BNNSs-OH/PMMA
Blank PMMA	1.87	1.87
0.1	1.91	5.85
0.5	2.67	5.74
1.5	1.11	3.26
2	0.74	3.69
5	0.82	3.18

Conclusions

In summary, functionalized the h-BN with sonication assisted exfoliation in deionized water using surfactant was successfully synthesized. AFM and SEM showed the nanosheets of 5 nm to 25 nm were successfully exfoliated with average lateral sizes of 1.11 µm to 1.67 µm. Enhanced mechanical and thermal properties showed that strong interactions between BNNS-OH/PMMA, which can be ascribed to hydrogen bonding. SEM images of nanocomposites revealed that the functionalization results in better dispersion. The mechanical properties showed the enhancement in tensile strength from 15.05 MPa for base polymer (PMMA) to 25.99 MPa at just 0.5 wt. % with an increase of 72 % for functionalized as compare to increase of 30 % for non-functionalized nanocomposites. Young's modulus increases 52 % and 40 % for functionalized and non- functionalized nanocomposites respectively. Strain at break also increases 212 % and 42 % for functionalized and non- functionalized nanocomposites respectively. These nanocomposites with enhance strength can be used for the development of structural components for structural applications.

Recommendations

Owing to enhance mechanical properties, these functionalized nanosheets (BNNSs-OH) can further be studied for applications such as thermal management using thermal conductivity, for electronic packaging applications, dielectric properties can be explored as BN is insulator and due to hydroxylic group attached to the surface of nanosheets, its use can be found in biomedical applications.

References

[1]   E. Gibney, "The super materials that could trump graphene," *Nature,* vol. 522, no. 7556, pp. 274-276, **2015.**

[2]   J. d. L. Fuente, "Graphene Applications & Uses," **2019.** Available: https://www.graphenea.com/pages/graphene-uses-applications#.XShw2m5uJMs

[3]   Grand View Research. Inc., "Graphene Market Size," **2019.** Available: https://www.grandviewresearch.com/press-release/global-graphene-market

[4]   Y. Lin and J. W Connell, "Advances in 2D boron nitride nanostructures: Nanosheets, nanoribbons, nanomeshes, and hybrids with graphene," *Nanoscale,* vol. 4, no. 22, pp. 6908-6939, **2012.**

[5]   A. Reports, "Global hexagonal boron nitride market analysis by trends, challenges and growth drivers analysis 2019-2023," **2019**. Available: https://portnews24.com/global-hexagonal-boron-nitride-market-analysis-by-trends-challenges-and-growth-drivers-analysis-2019-2023/83613/

[6]   X. Wang, C. Zhi, Q. Weng, Y. Bando, and D. Golberg, "Boron nitride nanosheets: Novel syntheses and applications in polymeric composites," *Journal of Physics: Conference Series,* vol. 471, no. 1, pp. 1-10, **2013**.

[7]   S. Fu, Z. Sun, P. Huang, Y. Li, and N. Hu, "Some basic aspects of polymer nanocomposites: A critical review," *Nano Materials Science,* vol. 1, no. 1, pp. 2-30, **2019.**

[8]   J. Silvestre, N. Silvestre, and J. de Brito, "Polymer nanocomposites for structural applications: Recent trends and new perspectives," *Mechanics of Advanced Materials and Structures,* vol. 23, no. 11, pp. 1263-1277, **2016.**

[9]   K. A. Dubey, P. A. Hassan, and Y. K. Bhardwaj, "Chapter 5: High Performance Polymer Nanocomposites for Structural Applications," in *Materials Under Extreme Conditions*, Amsterdam: Elsevier, 1st ed, pp. 159-194, **2017.**

[10]   K. I. Winey, R. A. Vaia, and G. Editors, "Polymer nanocomposite," *MRS Bulletin,* vol. 32, no. 4, pp. 314-322, **2007.**

[11]   R. Sierra-Ávila *et al.*, "Synthesis and thermomechanical characterization of Nylon 6/Cu nanocomposites produced by an ultrasound-assisted extrusion

method," *Advances in Materials Science and Engineering,* vol. 2018, no. 4792735, pp. 1-10, **2018.**

[12]   U. Ali, K. J. B. A. Karim, and N. A. Buang, "A review of the properties and applications of poly (methyl methacrylate) (PMMA)," *Polymer Reviews,* vol. 55, no. 4, pp. 678-705, **2015.**

[13]   R. Krishnamoorti, "Strategies for dispersing nanoparticles in polymers," *MRS Bulletin,* vol. 32, no. 4, pp. 341-347, **2007.**

[14]   L. S. Schadler, S. K. Kumar, B. C. Benicewicz, S. L. Lewis, and S. E. Harton, "Designed interfaces in polymer nanocomposites: A fundamental viewpoint," *MRS Bulletin,* vol. 32, no. 4, pp. 335-340, **2007.**

[15]   B. Marrs, R. Andrews, T. Rantell, and D. Pienkowski, "Augmentation of acrylic bone cement with multiwall carbon nanotubes," (in eng), *J Biomed Mater Res A,* vol. 77, no. 2, pp. 269-76, **2006.**

[16]   X.-L. Xie, Y. W. Mai, and X.-P. Zhou, "Dispersion and alignment of carbon nanotubes in polymer matrix: A review," *Materials Science and Engineering: R: Reports,* vol. 49, no. 4, pp. 89-112, **2005.**

[17]   H. Wu and M. R. Kessler, "Multifunctional cyanate ester nanocomposites reinforced by hexagonal boron nitride after noncovalent biomimetic functionalization," *ACS Applied Materials & Interfaces,* vol. 7, no. 10, pp. 5915-5926, **2015.**

[18]   S. Xie *et al.*, "Boron nitride nanosheets as barrier enhancing fillers in melt processed composites," *Nanoscale,* vol. 7, no. 10, pp. 4443-4450, **2015.**

[19]   X. Wu, H. Liu, Z. Tang, and B. Guo, "Scalable fabrication of thermally conductive elastomer/boron nitride nanosheets composites by slurry compounding," *Composites Science and Technology,* vol. 123, no. 8, pp. 179-186, **2016.**

[20]   R. Haggenmueller, H. Gommans, A. G. Rinzler, J. E. Fischer a, and K. Winey, "Aligned single-wall carbon nanotubes in composites by melt processing methods," *Chemical Physics Letters,* vol. 330, no. 3-4, pp. 219-225, **2000.**

[21]   F. Liu *et al.*, "Cheap, gram-scale fabrication of BN nanosheets via substitution reaction of graphite powders and their use for mechanical reinforcement of polymers," (in English), *Scientific Reports,* vol. 4, no. 4211, pp. 1-8, **2014.**

[22]   H. J. Ye *et al.*, "Liquid-phase exfoliation of hexagonal boron nitride into boron nitride nanosheets in common organic solvents with hyperbranched

polyethylene as stabilizer," (in English), *Macromolecular Chemistry and Physics,* vol. 219, no. 6, pp. 1-12, **2018.**

[23]   J. H. Yu, H. L. Mo, and P. K. Jiang, "Polymer/boron nitride nanosheet composite with high thermal conductivity and sufficient dielectric strength," (in English), *Polymers for Advanced Technologies,* vol. 26, no. 5, pp. 514-520, **2015.**

[24]   D. G. Ortiz *et al.*, "Development of novel h-BNNS/PVA porous membranes: Via pickering emulsion templating," *Green Chemistry,* vol. 20, no. 18, pp. 4319-4329, **2018.**

[25]   X. Huang *et al.*, "Thermally conductive, electrically insulating and melt-processable polystyrene/boron nitride nanocomposites prepared by in situ reversible addition fragmentation chain transfer polymerization," *Nanotechnology,* vol. 26, no. 1, pp. 1-10, **2015.**

[26]   L. L. Qin *et al.*, "Preparation, characterization, and thermal properties of poly (methyl methacrylate)/boron nitride composites by bulk polymerization," (in English), *Polymer Composites,* vol. 36, no. 9, pp. 1675-1684, **2015.**

[27]   J. Lee *et al.*, "Boron nitride nanosheets (bnnss) chemically modified by "grafting-from" polymerization of poly(caprolactone) for thermally conductive polymer composites," *Chemistry, an Asian Journal,* vol. 11, no. 13, pp. 1921-1928, **2016.**

[28]   S. K. Kumar, N. Jouault, B. Benicewicz, and T. Neely, "Nanocomposites with Polymer Grafted Nanoparticles," *Macromolecules,* vol. 46, no. 9, pp. 3199-3214, **2013.**

[29]   S. Iijima, "Helical microtubules of graphitic carbon," *Nature,* vol. 354, no. 6348, pp. 56-58, **1991.**

[30]   N. G. Chopra *et al.*, "Boron nitride nanotubes," (in eng), *Science,* vol. 269, no. 5226, pp. 966-973, **1995.**

[31]   Y. Jun Chen, H. Zhang, and Y. Chen, "Pure boron nitride nanowires produced from boron triiodide," *Nanotechnology,* vol. 17, no. 3, pp. 786-789, **2006.**

[32]   Y. Qiu *et al.*, "Synthesis of continuous boron nitride nanofibers by solution coating electrospun template fibers," (in eng), *Nanotechnology,* vol. 20, no. 34, pp. 185-188, **2009.**

[33] H. Zhang, J. Yu, Y. Chen, and J. Fitz Gerald, "Conical boron nitride nanorods synthesized via the ball-milling and annealing method," *Journal of the American Ceramic Society,* vol. 89, no. 2, pp. 675-679, **2006.**

[34] U. Khan, A. O'Neill, H. Porwal, P. May, K. Nawaz, and J. N. Coleman, "Size selection of dispersed, exfoliated graphene flakes by controlled centrifugation," *Carbon,* vol. 50, no. 2, pp. 470-475, **2012.**

[35] A. Pakdel, Y. Bando, and D. Golberg, "Nano boron nitride flatland," *Chemical Society Reviews,* vol. 43, no. 3, pp. 934-959, **2014.**

[36] G. Constantinescu, A. Kuc, and T. Heine, "The stacking in bulk and bilayer hexagonal boron nitride," *Physical Review Letters,* vol. 111, no. 3, pp. 1-10, **2013.**

[37] Q. Peng, W. Ji, and S. De, "Mechanical properties of the hexagonal boron nitride monolayer: Ab initio study," *Computational Materials Science,* vol. 56, no. 1, pp. 11-17, **2012.**

[38] W. Meng, Y. Huang, Y. Fu, Z. Wang, and C. Zhi, "Polymer composites of boron nitride nanotubes and nanosheets," *Journal of Materials Chemistry C,* vol. 2, no. 47, pp. 10049-10061, **2014.**

[39] C. R. Dean *et al.*, "Boron nitride substrates for high-quality graphene electronics," *Nature Nanotechnology,* vol. 5, no. 10, pp. 722–726, **2010.**

[40] D. Dikin *et al.*, "Preparation and characterization of graphene oxide paper," *Nature,* vol. 448, no. 7152, pp. 457-460, **2007.**

[41] C. Huo, Z. Yan, X. F. Song, and H. Zeng, "2D materials via liquid exfoliation: a review on fabrication and applications," *Science Bulletin,* vol. 60, no. 23, pp. 1994-2008, **2015.**

[42] Y. Hernandez, M. Lotya, D. Rickard, S. D. Bergin, and J. N. Coleman, "Measurement of multicomponent solubility parameters for graphene facilitates solvent discovery," *Langmuir,* vol. 26, no. 5, pp. 3208-3213, **2010.**

[43] C. Y. Zhi *et al.*, "Mechanical and thermal properties of polymethyl methacrylate-BN nanotube composites," (in English), *Journal of Nanomaterials,* vol. 1, no. 5, pp. 1-5, **2008.**

[44] J. M. Hughes, D. Aherne, and J. N. Coleman, "Generalizing solubility parameter theory to apply to one- and two-dimensional solutes and to incorporate dipolar interactions," *Journal of Applied Polymer Science,* vol. 127, no. 6, pp. 4483-4491, **2013.**

[45] J. N. Coleman, "Liquid-phase exfoliation of nanotubes and graphene," *Advanced Functional Materials*, vol. 19, no. 23, pp. 3680-3695, **2009.**

[46] A. C. Ferrari and F. Bonaccorso, "Science and technology roadmap for graphene, related two-dimensional crystals, and hybrid systems " *Nanoscale,* vol. 7, no. 11, pp. 4587-4587, **2015.**

[47] A. Chae, S. J. Park, B. Min, and I. In, "Enhanced dispersion of boron nitride nanosheets in aqueous media by using bile acid-based surfactants," (in English), *Materials Research Express,* vol. 5, no. 1, pp. 1-8, **2018.**

[48] A. A. Green and M. C. Hersam, "Solution phase production of graphene with controlled thickness via density differentiation," *Nano Letters,* vol. 9, no. 12, pp. 4031-4036, **2009.**

[49] J. Shen *et al.*, "Liquid phase exfoliation of two-dimensional materials by directly probing and matching surface tension components," *Nano Letters,* vol. 15, no. 8, pp. 5449-5454, **2015.**

[50] P. May, U. Khan, A. O'Neill, and J. N. Coleman, "Approaching the theoretical limit for reinforcing polymers with graphene," *Journal of Materials Chemistry,* vol. 22, no. 4, pp. 1278-1282, **2012.**

[51] W. D. Callister and W. D. C. William D., *Materials Science and Engineering: An Introduction*, University of Michigan, USA: John Wiley & Sons, Limited, 8th ed., pp. 452-500, **2007.**

[52] L. Gong *et al.*, "Optimizing the reinforcement of polymer-based nanocomposites by graphene," (in eng), *ACS Nano,* vol. 6, no. 3, pp. 2086-2095, **2012.**

[53] H. Raza, *Graphene nanoelectronics: Metrology, synthesis, properties and applications*, Iowa City, USA: Springer Science & Business Media, 1st ed., pp. 93-134, **2012.**

[54] H. Xu, B. W. Zeiger, and K. S. Suslick, "Sonochemical synthesis of nanomaterials," *Chemical Society Reviews,* vol. 42, no. 7, pp. 2555-2567, **2013.**

[55] K. S. Novoselov *et al.*, "Electric field effect in atomically thin carbon films," *Science,* vol. 306, no. 5696, pp. 666-669, **2004.**

[56] D. Pacilé, J. C. Meyer, Ç. Ö. Girit, and A. Zettl, "The two-dimensional phase of boron nitride: Few-atomic-layer sheets and suspended membranes," *Applied Physics Letters,* vol. 92, no. 13, pp. 1-3, **2008.**

[57] C. Lee *et al.*, "Frictional characteristics of atomically thin sheets," *Science,* vol. 328, no. 5974, pp. 76-80, **2010.**

[58] L. H. Li, Y. Chen, G. Behan, H. Z. Zhang, M. Petravic, and A. M. Glushenkov, "Large-scale mechanical peeling of boron nitride nanosheets by low-energy ball milling," (in English), *Journal of Materials Chemistry,* vol. 21, no. 32, pp. 11862-11866, **2011.**

[59] T. Morishita and H. Okamoto, "Facile exfoliation and noncovalent superacid functionalization of boron nitride nanosheets and their use for highly thermally conductive and electrically insulating polymer nanocomposites," (in English), *ACS Applied Materials & Interfaces,* vol. 8, no. 40, pp. 27064-27073, **2016.**

[60] J. W. Wang *et al.*, "Noncovalent functionalization of boron nitride and its effect on the thermal conductivity of polycarbonate composites," (in English), *Journal of Applied Polymer Science,* vol. 134, no. 25, pp. 44978 (1-9), **2017.**

[61] G. R. Bhimanapati, D. Kozuch, and J. A. Robinson, "Large-scale synthesis and functionalization of hexagonal boron nitride nanosheets," (in English), *Nanoscale,* vol. 6, no. 20, pp. 11671-11675, **2014.**

[62] L. Cao, S. Emami, and K. Lafdi, "Large-scale exfoliation of hexagonal boron nitride nanosheets in liquid phase," (in English), *Materials Express,* vol. 4, no. 2, pp. 165-171, **2014.**

[63] K. Huang *et al.*, "Aminopolymer functionalization of boron nitride nanosheets for highly efficient capture of carbon dioxide," (in English), *Journal of Materials Chemistry A,* vol. 5, no. 31, pp. 16241-16248, **2017.**

[64] T. Sainsbury *et al.*, "Dibromocarbene functionalization of boron nitride nanosheets: Toward band gap manipulation and nanocomposite applications," *Chemistry of Materials,* vol. 26, no. 24, pp. 7039-7050, **2014.**

[65] T. Sainsbury *et al.*, "Covalently functionalized hexagonal boron nitride nanosheets by nitrene addition," *Chemistry-A European Journal,* vol. 18, no. 13, pp. 10808-10812, **2012.**

[66] R. Jan *et al.*, "Enhancing the mechanical properties of BN nanosheet-polymer composites by uniaxial drawing," *Nanoscale,* vol. 6, no. 9, pp. 4889-48895, **2014.**

[67] D. Louër, "Powder X-Ray Diffraction, Applications," in *Encyclopedia of Spectroscopy and Spectrometry*, J. C. Lindon, London, UK: Elsevier, 3rd ed., pp. 1865-1875, **1999.**

[68]   M. Abd Mutalib *et al.*, "Chapter 9: Scanning electron microscopy (SEM) and energy-dispersive X-ray (EDX) spectroscopy," in *Membrane Characterization*, Swansea University, UK: Elsevier, 1st ed., pp. 161-179, **2017.**

[69]   C. W. Oatley, W. C. Nixon, and R. F. W. Pease, "Scanning Electron Microscopy," in *Advances in Electronics and Electron Physics*, L. Marton, Ed. London, UK: Academic Press, vol. 21, pp. 181-247, **1966.**

[70]   M. S. Rana, H. R. Pota, and I. R. Petersen, "Improvement in the Imaging Performance of Atomic Force Microscopy: A Survey," *IEEE Transactions on Automation Science and Engineering,* vol. 14, no. 2, pp. 1265-1285, **2017.**

[71]   B. C. Smith, "Fundamentals of Fourier Transform Infrared Spectroscopy," Florida, United States, U.S.: CRC Press, 2nd ed., pp. 1-49, **2011.**

[72]   G. Höhne, W. F. Hemminger, and H. J. Flammersheim, *Differential Scanning Calorimetry*, Springer Berlin Heidelberg, 2nd ed., pp. 31-63, **2003.**

[73]   B. Wetzel, F. Haupert, and M. Qiu Zhang, "Epoxy nanocomposites with high mechanical and tribological performance," *Composites Science and Technology,* vol. 63, no. 14, pp. 2055-2067, **2003.**

[74]   H. Behniafar and S. Azadeh, "Transparent and flexible films of thermoplastic polyurethanes incorporated by nano-SiO_2 modified with 4,4′-methylene diphenyl diisocyanate," *International Journal of Polymeric Materials and Polymeric Biomaterials,* vol. 64, no. 1, pp. 1-6, **2015.**

[75]   N. Patra, A. C. Barone, and M. Salerno, "Solvent effects on the thermal and mechanical properties of poly(methyl methacrylate) casted from concentrated solutions," *Advances in Polymer Technology,* vol. 30, no. 1, pp. 12-20, **2011.**

[76]   H. M. F. Shakir, A. Tariq, A. Afzal, and I. Abdul Rashid, "Mechanical, thermal and EMI shielding study of electrically conductive polymeric hybrid nano-composites," *Journal of Materials Science: Materials in Electronics,* vol. 30, no. 18, pp. 17382-17392, **2019.**